Effect Of Power Control in Forwarding Strategies for Wireless Ad-Hoc Networks

Pratik Pareek,Aditya Kawatra

May 12, 2008

Certification

This is to certify that the project entitled ***'Effect Of Power Control in Forwarding Strategies for Wireless Ad-Hoc Networks'*** being submitted by **Pratik Pareek and Aditya Kawatra**, on the completion of their B.Tech Project in the Dept. of Electrical Engineering, Indian Institute of Technology, New Delhi is a record of bonafide work done by them under my supervision and guidance.

Prof Swades De
Dept of Electrical Engineering
Indian Institute of Technology
New Delhi - 110016
India
Date:

Acknowledgements

We would like to express our deep and sincere gratitude to our supervisor Dr. Swades De, Dept. of Electrical Engg. His wide knowledge and his logical thinking has been a great value for us. His understanding , encouraging and personal guidance has provided a good basis for the present thesis.

Aditya Kawatra,
Pratik Pareek,
IIT Delhi.

Abstract

This project aims to study the interference effects of neighboring nodes in one hop transmissions for Wireless AD-HOC networks. Previous work in this area has given results for a probabilistic value of the interference effect at a transmitting node for the major transmission strategies - NFP (Nearest with most Forward Progress), MFR (Most forward with Fixed Radius) and MVR (Most forward with Variable Radius). But, a major source of interference which are the nodes outside the transmission radius but within the interference radius (called the Interference Zone) have not been captured. These nodes can sense a transmission (but not decode it) and have enough noise power to garble the signal received at the actual receiving node. The number of potential interfering nodes has been estimated. Also an expression for the probabilistic interference power due to these nodes at the receiver has been obtained, for each 'n' (number of interfering nodes). Since the closed form expressions are difficult to evaluate, computer aided computations have been carried out to estimate the interference and SIR (Signal to Interference Ratio) values, for non-power control as well as for power control (NFP, MVR and Random). We confirmed our analytical results with a Brute-Force simulation.

Also, parameters like Transmission Power utilized per unit distance between transmitter and receiver and the corresponding device power used have been evaluated for the three transmission strategies. We have also compared these parameters for different values of Node Density and ranked their performances on this basis.

Contents

List of Figures

Chapter 1

Introduction

1.1 AD HOC Networks

1.1.1 Basics

A wireless ad hoc network is a decentralized wireless network. Operating in ad-hoc mode allows all wireless devices within range of each other to discover and communicate in peer-to-peer fashion without involving central access points The network is ad hoc because each node is willing to forward data for other nodes, and so the determination of which nodes forward data is made dynamically based on the network connectivity. This is in contrast to wired networks in which routers perform the task of routing. It is also in contrast to managed wireless networks, in which a special node known as an access point manages communication among other nodes.

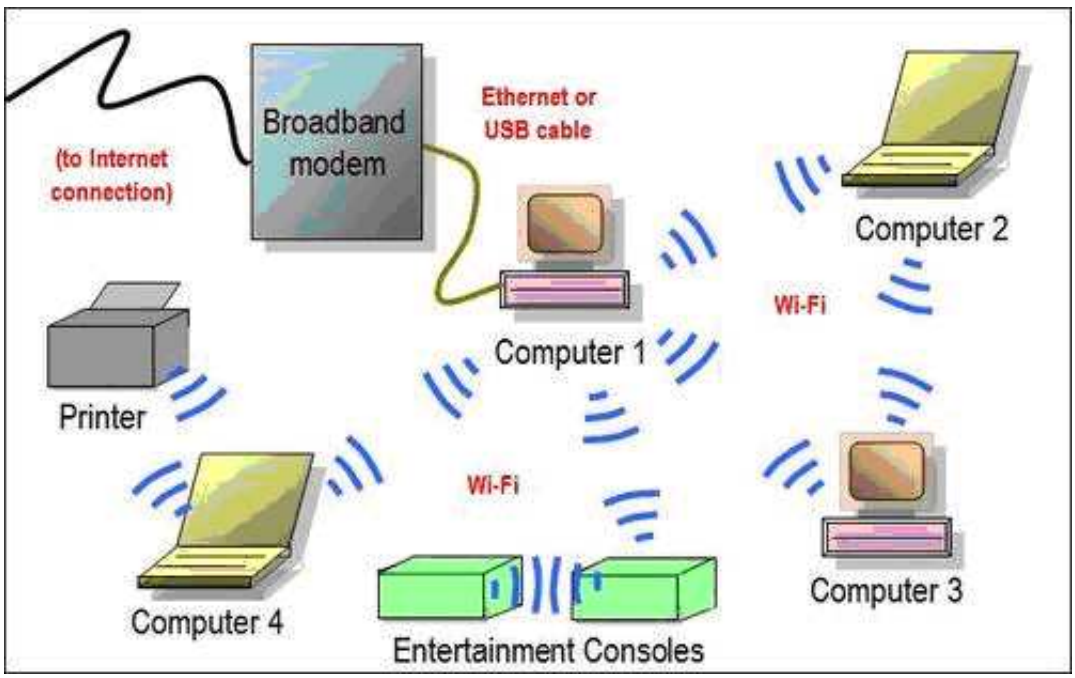

Figure 1.1: A typical example of Wireless AD Hoc Network in Computer Networks

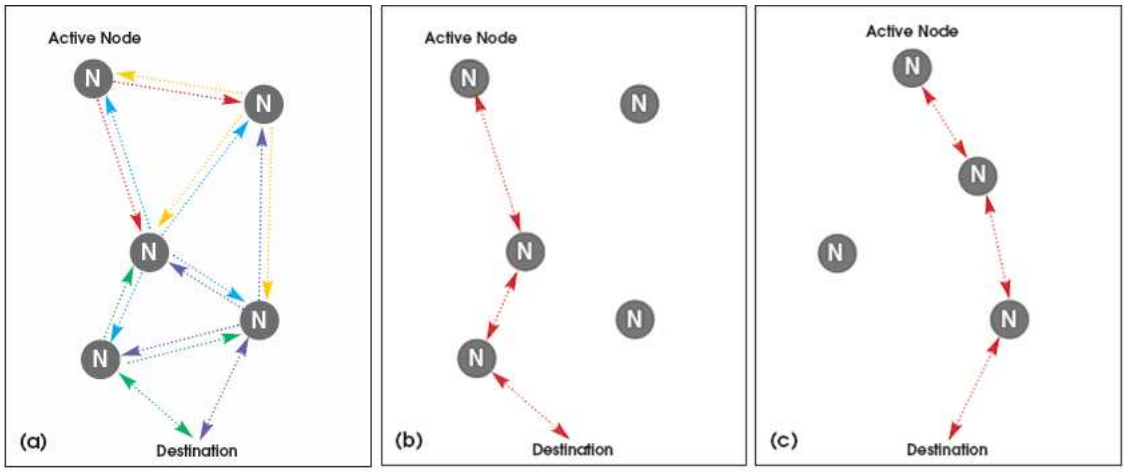

The term mesh network accurately describes the structure of the network: All available nodes are aware of all other nodes within range. The entire collection of nodes is interconnected in many different ways, just as a physical mesh is made of many small connections to create a larger fabric. Figure 1 provides a simple diagram illustrating these concepts. This diagram is modeled after a wireless ”hot spot,” where an ad hoc network links users to a router with access to the Internet. In this example, two users are highlighted, showing two paths through several nodes to the router. If one of the intermediate nodes were to fail (e.g. that user leaves the area), the network will automatically reconfigure itself, locating an alternate path from the user to the router. Typically, all available nodes are also network users, each sharing the total data transfer capacity of the particular hardware and operating protocol being used. The network could also connect users to other users directly, as would be done in an industrial control and monitoring network. Since there is no need for central administration of the network configuration, it is most efficient to design the system for autonomous operation of each node. In an industrial environment, a situation such as an alarm would be propagated through the network and received directly by each node. Each node would be programmed to respond according to its particular function- machine control, process monitoring, supervisory personnel or central office.

1.1.2 Self-Configuring and Self-Healing Processes

Figure 2 shows how ad hoc networks determine their configuration. In Fig. 2(a) each node identifies the nodes that are available for communications, based on signal strength, which is mainly related to distance, but is also affected by obstructions or interference. Some nodes may be beyond range, others may be detectable but have insufficient signal strength for reliable communications. Once the available nodes are identified, this information is communicated to other nodes, along with information about the desired destination (Fig. 2b). Using the lists of available connections, the network configuration algorithm selects a particular routing for each user to its destination. This process requires system operating software to have good decision-making algorithms, based on practical criteria for signal strength, path reliability over time, and network configuration patterns. Over time, or even near-continuously, the network will change.

Users may come and go, nodes may be in motion, or changes in the electromagnetic envi-

ronment may alter the propagation between nodes. As these changes take place, the network will update its configuration and identify new paths from users to destinations, as illustrated in Fig. 2c. This type of reconfiguration will be repeated over and over as the network changes. Note that this is the same process used in the Internet, where system loading and hardware issues require redirection of a user's data through different routers.

1.1.3 Advantages of Ad Hoc Networks

The principal advantages of an ad hoc network include the following:

- Independence from central network administration.
- Self-configuring, nodes are also routers.
- Self-healing through continuous re-configuration.
- Scalable-accommodates the addition of more nodes
- Flexible-similar to being able to access the Internet from many different locations

1.1.4 Limitations of Ad Hoc Networks

While ad hoc networks are typically used where they have the greatest emphasis on its advantages, there are some limitations:

- Each node must have full performance
- Throughput is affected by system loading
- Reliability requires a sufficient number of available nodes. Sparse networks can have problems
- Large networks can have excessive latency (time delay), which affects some applications Some of these limitations also apply to conventional hub-and-spoke based networks, or cannot be addressed by alternate configurations. For example, all networks are affected by system loading, and networks with few nodes are difficult to justify in hard-wired solutions.

1.1.5 Key Applications

The decentralized nature of wireless ad hoc networks makes them suitable for a variety of applications where central nodes cannot be relied on, and may improve the scalability of wireless ad hoc networks compared to wireless managed networks, though theoretical and practical limits to the overall capacity of such networks have been identified.

WLAN is the initial application that received a concerted development effort. Peer-to-peer networks of computer/ PDA users have become common. Commercial wireless Internet service providers (WISP) use repeater nodes to extend coverage to a large area, while user nodes can extend service in their locality. Control systems (e.g. environmental controls) and industrial process monitoring and control are becoming major applications for mesh networking. These

environments are difficult to serve with dedicated wiring, being spread over a large area, often with difficult access. Sensor networks from small-scale (e.g. household security monitoring) to large scale (e.g. wildlife tracking) are also being developed with ad hoc networking as the operational structure. Developers of these and other applications have determined that ad hoc networks are the most efficient way to maintain system-wide communications.

1.2 The Slotted Aloha Protocol

1.2.1 Basics

In the seventies, the ALOHA system was proposed by Norman Abramson as an effective solution to provide for wireless access to computer systems. The ALOHA-net at the University of Hawaii employed fixed transmitters at islands located at ranges of several tens of kilometers. The main advantage of the ALOHA random access scheme was simplicity. Terminals can transmit their data regardless of the activity of other terminals. If a message is successful the base station sends an acknowledgement over a feedback channel. If the terminal does not received an acknowledgement, the terminal retransmits the message after waiting a random time. The delay is mainly determined by the probability that a packet is not received (because of interference from another transmission, called a ”collision”) and the average value of the random waiting time before a retransmission is made.

1.2.2 Collision Resolution

Later studies revealed that, for an infinite population of users and under certain channel conditions, the ALOHA system is unstable. Packets lost in a collision are retransmitted, but the retransmission again experiences a collision. This may set off an avalanche of retransmission attempts. Almost surely, the ”backlog”, i.e., the number of previously unsuccessful packets that need to be retransmitted, grows beyond any finite bound. One method to mitigate instability is to dynamically adapt the random waiting times of all terminals if the base station notices that many collisions occur. Examples of methods to ensure stability are Dynamic Frame Length (DFL) ALOHA, by Frits Schoute, or the Stack Algorithm by Boris Tsybakov et al. DFL uses a centralized control, mastered by the base station, while the stack algorithm is a decentralized method.

1.2.3 ALOHA in Mobile Radio Networks

The ALOHA concept is very commonly used in modern wireless communication systems. The call set-up procedure of almost any (analog or digital) cellular telephone system uses some kind of ALOHA random access. But the performance differs from what one would expect in a wireline network.

In a radio channel, packets may be lost because of signal fading even if no contending other signal is present. On the other hand, packets may be received successfully despite interference from competing terminals. This is called ‘receiver capture’. This effect has a significant influence on the throughput. Optimum frequency reuse for ALOHA Random Access networks differs from frequency reuse for telephony, because the performance criteria differ (throughput / delay versus outage probability, respectively). The best reuse pattern for an ALOHA system is to use the same frequency in all cells.

1.2.4 The ALOHA Principal

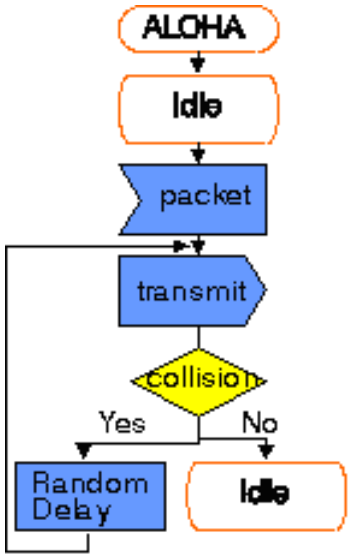

Figure 1.2: Description of terminal behavior in ALOHA random access network

In unslotted ALOHA, a transmission may start at any time. In slotted ALOHA the time axis is divided to slots. All terminals are assumed to know the times at which a new slot begins. Packets may only be transmitted at the beginning of a new slot. Slotted ALOHA has significantly better throughput than unslotted ALOHA.

1.2.5 Performance

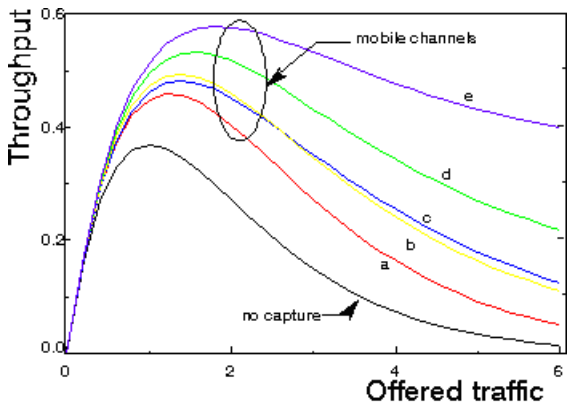

Figure 1.3: Throughput S of Slotted ALOHA network (in packet per time slot) versus the attempted traffic.

1.3 Current state of art

As of now, the current forwarding strategies used for transmission have been analyzed and compared with each other on the basis of certain parameters [1]. This paper has assumed the following network model-

- The nodes are distributed as a two-dimensional Poisson point process with density λ, i.e the Pr(finding i nodes in an area of size A) =

$$\frac{\lambda A i e^{-\lambda A}}{i!}$$

  Where, i=0,1,2,3..

- The channel access protocol is slotted ALOHA. The traffic is assumed to be uniform, i.e., every node transmits to every other node with equal probability and every node has equal traffic load.

- Each node transmits with a maximum radius R. The quantity N= $\lambda \mathrm{p} R^2$ represents the average number of neighbors of a node. A successful transmission occurs from X to Y if Y does not transmit and Y's neighbors do not interfere with Y (i.e do not transmit in the same slot).

Forward progress is defined as the projection of the vector from a transmitting node to its immediate one-hop receiver onto the vector from the transmitter to the final destination (can be positive or negative). An important transmission rule is that one-hop transmissions with negative forward progress are not allowed.

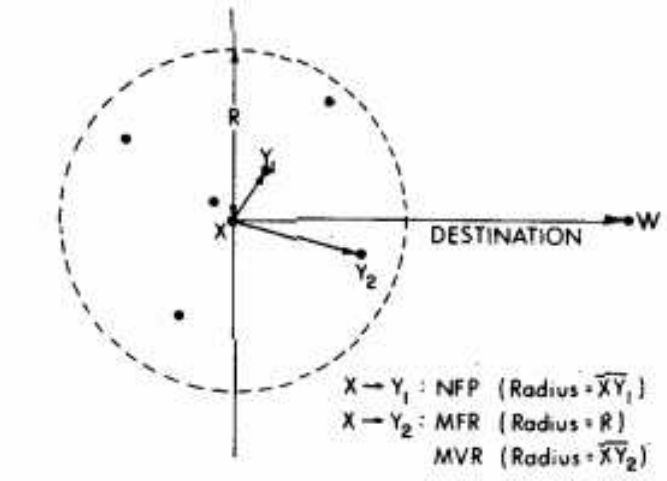

Figure 1.4: Illustration of Transmission Strategies

The major forwarding strategies are-

- NFP (Nearest forward Progress) A node transmits to the nearest neighbor which will result in forward progress. The transmission power is adjusted to be just strong enough to reach the receiving node. The aim is to reduce conflicts as far as possible. If we

represent the distance between a transmitter (X) and its immediate receiver (Y) with the random variable r, then $f_r(r_0)$ is given by

$$f_r(r_0) = \frac{\lambda \pi r_0 e^{\lambda \pi r_0^2/2}}{1 - e^{-N/2}}, \qquad 0 \leq r_0 \leq R \tag{1.1}$$

- MFR (Most Forward with Fixed Radius R) A node transmits to a neighbor with the largest forward progress. The transmission radius is fixed at R in this strategy irrespective of the position of the receiving node. The aim is to minimize the number of hops needed for a packet to reach its destination.
- MVR (Most Forward with Variable Radius) This strategy is similar to MFR except that the transmission radius is adjusted to be equal to the actual distance between the transmitter and the receiver. Thus the aim is to combine the benefits of the previous two strategies, i.e. to reduce the conflict to some extent while achieving the largest progress possible.

The expression for $f_r(r_0)$ for both MFR and MVR is the same and is given by

$$f_{r,\theta}(r_0, \theta_0) = \frac{\lambda r_0 e^{-\lambda A_Z}}{1 - e^{-N/2}}, \qquad 0 \leq r_0 \leq R, -\pi/2 \leq \theta_0 \leq \pi/2 \tag{1.2}$$

where,

$$A_Z = R^2(cos^{-1}[(r_0/R)cos(\theta_0)] - (r_0/R)cos(\theta_0)\sqrt{1 - [r_0 cos\theta_0/R]^2}) \tag{1.3}$$

The final results were obtained for the following parameters-

S = local throughput (one hop throughput) = average number of transmissions per slot from a node.

Z = average progress per slot from a transmitting node.

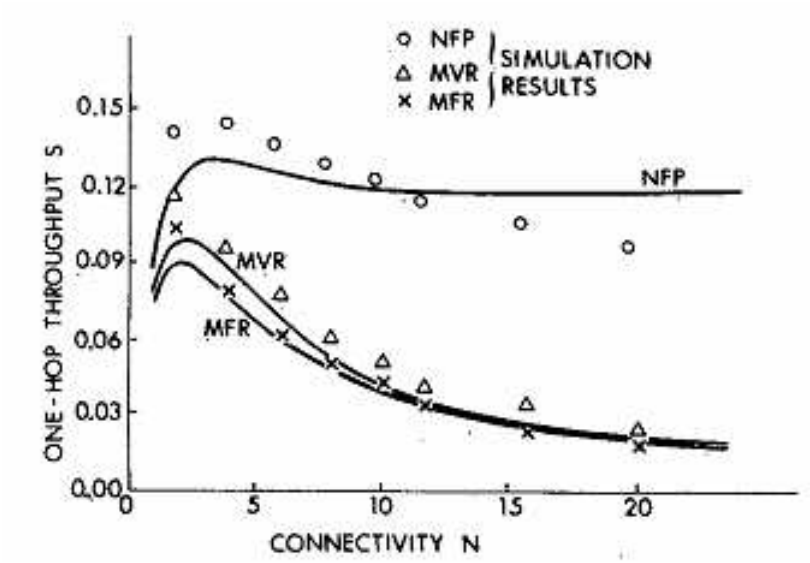

Figure 1.5: One Hop throughput S versus connectivity N

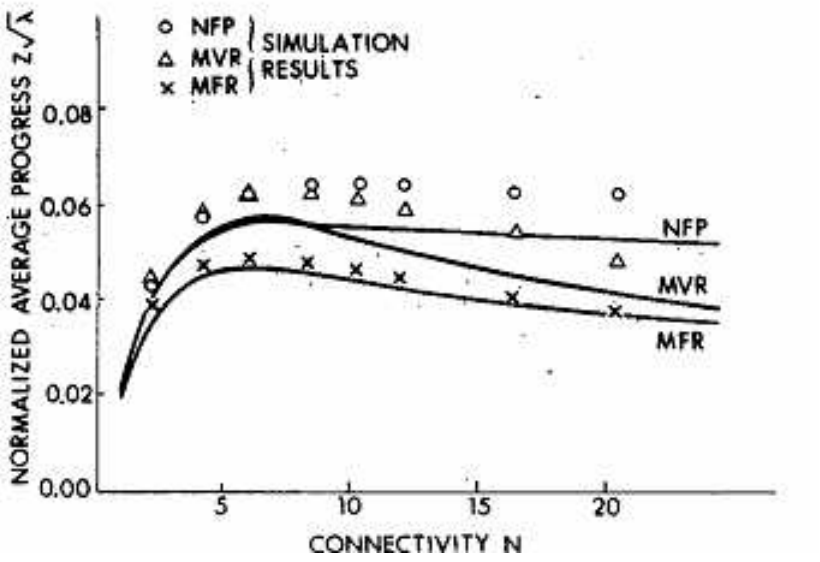

Figure 1.6: Normalized average progress Z_n, versus connectivity N

Chapter 2

Interference Zone Effects

2.1 Explanation

The transmission power from any transmitting node does not completely diminish after the intended transmission radius. Instead, the signal propagates further until a certain greater distance and decays down to a power level below which it is imperceptible to the sensors (around the channel noise power level). This maximum range is called the interference radius and it is found to be approximately equal to twice the transmission radius for most wireless networks (i.e. R_I=2*R_T). The ring region from the transmission radius to the interference radius is called the interference zone or the carrier sensing zone. In this region of a particular transmitter, the neighboring nodes cannot decode the transmission signal and can only sense the signal carrier (used for modulation).

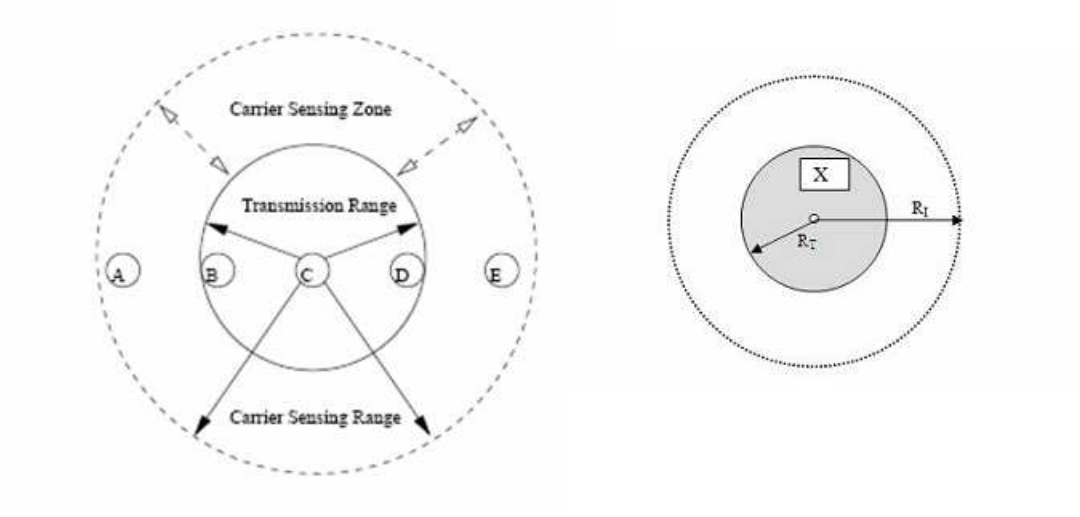

Figure 2.1: The Solid circle is the transmission zone (of radius R_T) and the dotted circle is the interference zone boundary (of radius R_I)

Thus the interference zone nodes of a receiver will add further (quantitatively) to the interference at it. This is because, in the absence of a RTS-CTS protocol, the interference zone nodes of a receiver (say Y) cannot sense the transmission from the main transmitting node (say

X), thus becoming something of a hidden zone for X. Even under the RTS-CTS protocol, the mechanism needs to be properly synchronized for the hidden nodes to keep quiet. The exposed terminal zone problem doesn't come in here as the interference zone is not very large. But if some wireless network models have larger carrier sensing zones, then this problem might come in to the picture. The effective interference zone for Y is shown below in the figure. All nodes in this shaded area can potentially interfere with the intended signal at Y if they too are transmitting. In quantitative terms, if such nodes transmit at reasonable power (as given by the forwarding strategy), the resulting SINR at the receiver could be small enough to cause decoding errors.

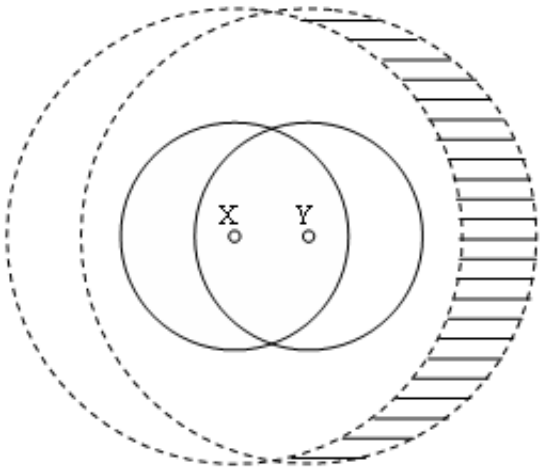

Figure 2.2: The shaded region is the effective interference zone for Y

2.2 Assumptions

Thus the basic assumptions for our study are the following-

- The transmission protocol for the network can be taken to be slotted ALOHA (as in [1]) with Carrier Sense Multiple Access (CSMA without collision detection). The antennas used in the network are isotropic.
- The basic assumptions in [1] (as mentioned in the introduction), apart from the fact that we allow backward transmissions in case of all the power control strategies. This is a necessary clause for calculating the interference from the interfering nodes, since their individual directions of transmissions can be random and it would be unviable to consider all possible directions (explained further in the power control chapter i.e Chapter 4).
- The time lag between a data transmission and a neighboring node sensing it is assumed to be lesser than the fixed time slot of the protocol i.e. both the receiver node and the interference zone nodes will sense the transmission within the same time slot as that of the data transmission and the transmission and interference nodes will keep quiet from the next slot onwards, till the length of the transmission. Also, the amount of interference estimated is valid for one slot only.

- The effective interference zone nodes (shaded area) can also keep quiet if nodes from outside transmit, i.e. they can fall in the interference area of some external transmitting node. This possibility is ignored as we want to conduct a worst-case analysis anyways.

Chapter 3

3-node analysis (Non-Power Control)

3.1 Explanation

Our preliminary approach to estimating the interference at Y, was to estimate the total interference and SIR at Y effectively due to 3 nodes only. It might seem that the maximum number of interfering nodes could be very large, in case of a non-power control scheme. But this is not true. If we ignore for now the possibility of two or more nodes transmitting at the same instant (the probability of which is small), the maximum number of interfering nodes seems to be three.

This can be seen from the figure. The total shaded region is the effective interference zone. If a node at N_0 transmits (located in the total shaded region), then only nodes in area A_1 and A_2 can transmit which lie outside the interference zone of N_0. If N_0 is placed such that A_1 or A_2 vanish, there will be two interfering nodes. Thus the minimum number of interfering nodes is one (which happens either if there is only one node in the total shaded region or if the nodes in A_1 and A_2 do not transmit in the time-slot concerned) and the maximum number is three. We now aim to determine the condition for the effective interference of three nodes. If the node N_0, which lies approximately in the middle sector of the total shaded region, is confined to a certain sub-region then three nodes can be shown to exist. This is given by the region A_0 (curvilinear region given by S_1S_2 S_4S_3) in the figure. These points are determined by the intersection of the interference circles drawn at P_1 and P_2 and the interference circles for X and Y. The points P_1 and P_2 are the intersection points of the interference circles of X and Y. If a node happens to fall in A_0, then there is definitely a probability of two other interfering nodes, in the regions A_1 and A_2. The regions A_1 and A_2 are mutually exclusive in the sense that a node in either area will definitely be outside of the interference zone of a node in the other area. This we refer to as the 3-node case. The steps required to determine the probabilistic expected interference of such a case at Y are:

- Annular rings of thickness dr are drawn from Y, starting from radius Y S_1 to Y S_2 (=R_I). In each of these rings, elemental regions of area (using usual cylindrical coordinates convention) are taken and the probability of finding exactly one node in this area is computed. This node is N_O (Refer to Fig.3.1). The probabilistic interference at Y from N_O is thus given by

$$P_0 = p_t.pr, \alpha_1.P_T/r^n \tag{3.1}$$

  Where,

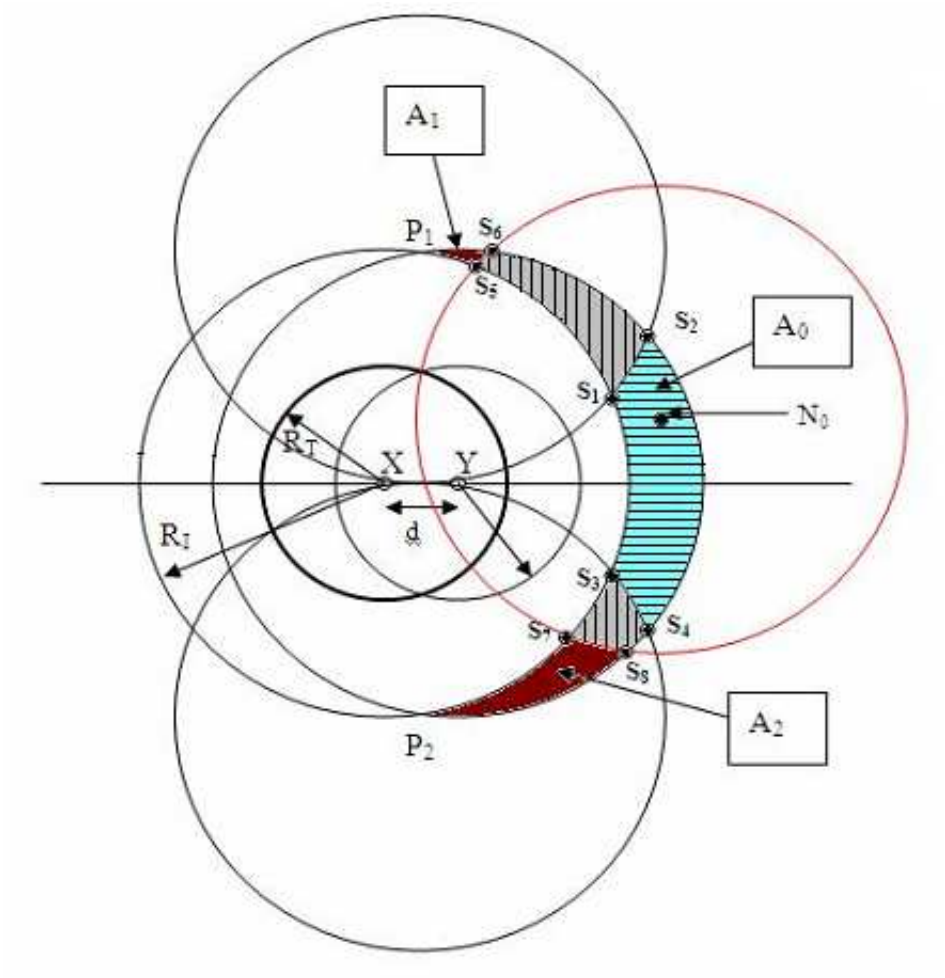

Figure 3.1: Interference circles for various transmitting nodes. Node X is transmitting to Y. All the shaded and striped regions together comprise the effective interference region for Y, determined by interference radius R_I

$p(r,\alpha)_1 = e^{-\lambda dA}\lambda dA$, is the probability of one node (given by Poisson's distribution) in the elemental area located at (r,α) ,

P_T is the full transmission power and 'n' is the path loss factor (typically between 2 and 3),

P_t is the transmission probability of any node in a time-slot.

Since, A_O is symmetric about line XY it suffices to only consider the area above and multiply the total interference calculated in this area by two. Note that the probability of finding two nodes in the element area, $p(r,\alpha)_2$ is given by

$$p(r,\alpha)_2 = e^{-\lambda dA}\lambda dA^2/2 = (1-\lambda dA+\lambda dA^2/2.....)\lambda dA^2/2 = \lambda dA^2/2-\lambda dA^3/2+..... \quad (3.2)$$

Thus, till a first degree approximation, this can be taken to be zero. Also note that $YS_1 \geq R_T - d$, thus the annular rings with radius variation from R_T - d to YS_1 were taken separately.

- For each N_0 its corresponding interference circle is drawn and A_0 and A_2 are determined by integration/numerical methods. As with N_0, annular rings are drawn in A_1 with Y as centre, starting from radius YS_5 upto YP_1 (=R_I). This radius variable is denoted by variable s (say) i.e $YS_5 \leq$ s $\leq R_I$. The angular span of any ring in A_1 is clearly a function of r,α and s. The probabilistic interference at Y due to a node in this region is then calculated (similar to expression for node N_0). This is integrated over all possible nodes in A_1. The expression finally reduces to a function of A_1, r and α only. Similar calculations are carried out for nodes in A_2. The 3-node sets produced by this method are all unique as N_0 is different for every iteration. They are exhaustive too.

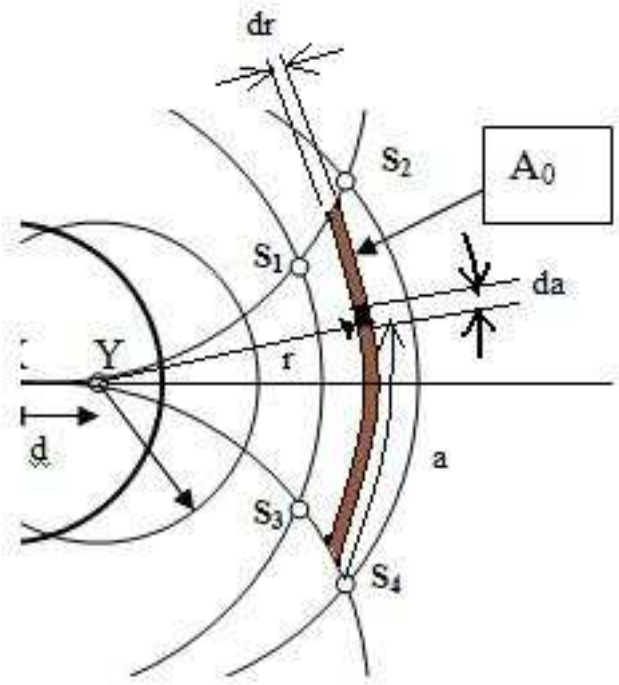

Figure 3.2: The elemantal area taken at a distance r from Y and angle α from the reference on curve S_3S_4

NOTE that there is a probability, although small, of there being four interfering nodes given that there are four or more nodes in the total shaded region. This happens when node N_0 is located at the fringes of the boundary line S_1S_2 or S_3S_4, as shown in Fig 4. Clearly, there are four possible interfering nodes, they being N_0, N_2 and one each in A_1 and A_3 (Fig.4. on page below). But both areas are, in general, extremely small and contribute a negligibly small probabilistic interference at Y. Note that the region A_3 is still considered overall in the 3-node analysis but it is counted as part of A_0, thus the interference calculation is an underestimation of the actual interference value. One can separate the two cases by taking a node N_0 (above XY line) for which x-coordinate of $S_8 \leq$ x-coordinate of S_4 (according to Fig.2), since only then will the area A_3 not come into the picture. The 4-node case can then be considered separately for those nodes (N_0) for which A_3 exists.

There will also be 2-node only cases. Either of the two nodes will not be in region A_0 (because then A_1 and A_2 will exist and there will be a probabilistic contribution from there

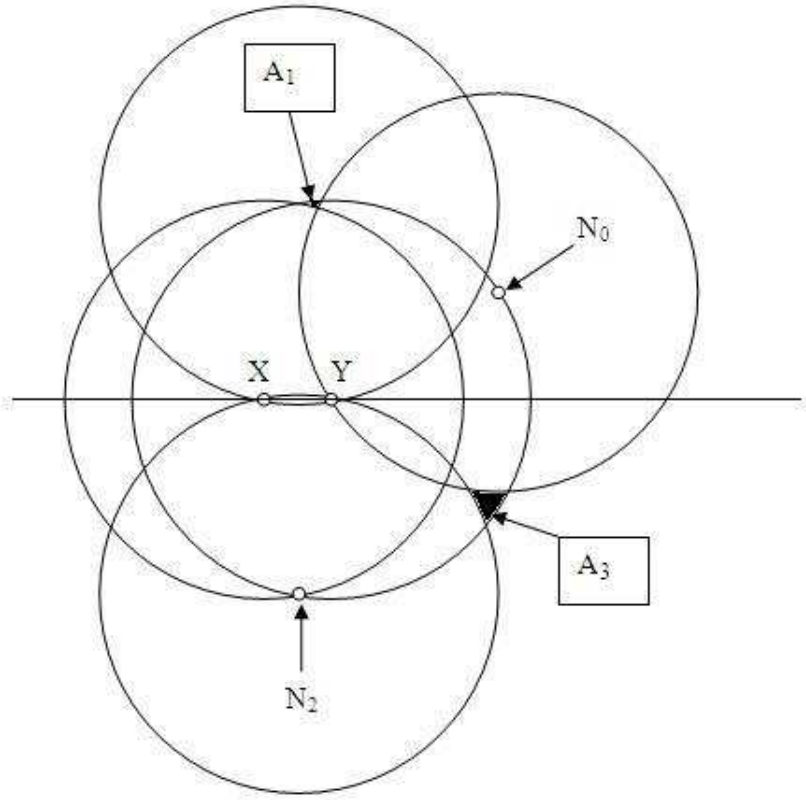

Figure 3.3: N_0 lies at the fringe of fixed area A_0. A_1 is the usual upper excluded area and P_2 is selected as N_2 in area A_2. We see that there is still a left over area A_3

also). The 3-node cases cover all of the two node cases along with a third node. Since, we are primarily concerned with a worst case analysis, the 2-node scenario doesn't need to be considered separately.

3.2 Numerical Simulation

For simulation, the value of d was varied from 0.1R_I to 0.45R_I because we have the constraint $d \leq R_T$ and R_T = 0.5R_I. MATLAB provides a tool to solve simultaneous equations of any kind, and this has been utilized in the simulation $(fsolvefunction)$. This tool was also used to verify the results for the coordinates obtained by manual calculations. Also, the $quadfunction$ was used to calculate definite integrals for calculating the areas A, A_0, A_1 and A_2. The path-loss factor (n) was taken to be 3.The total probabilistic interference and SIR were calculated for each value of d and results were plotted as follows : The relevant quantities are : Path loss factor 'n' = 3, δr = (R_I - YS_1)/100, $\delta\alpha$ = g(r)/50, α is the angle span of a ring and is from 0 to g(r) for a particular value of r.

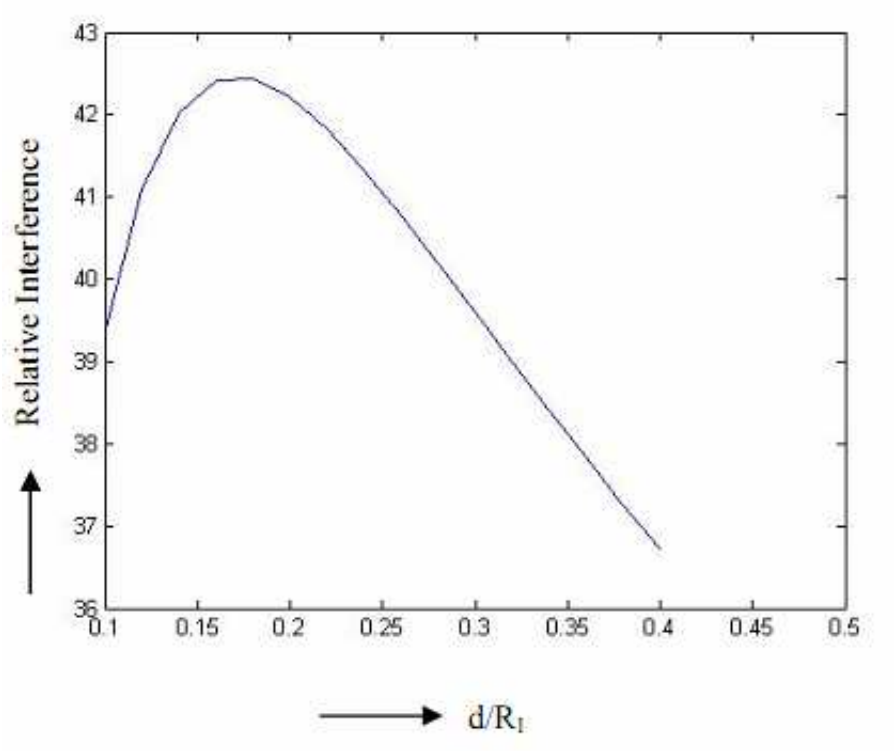

Figure 3.4: Interference vs d/ R_I

And the SIR curve was obtained as follows :-

The plot of I vs d/R_I can be interpreted as follows: When d is small, the effective interference region is small in size and therefore the number of potentially interfering nodes is less. Thus the interference is low. As d increases, the size of this region increases further, thus increasing the number of potential interferers and hence the total interference. But at the same time, the distance of the interfering nodes from Y also keeps on increasing. This results in a decrease of the total interference at Y, which becomes more and more evident as d keeps on increasing. At a particular value of d, I reaches a maximum which is approximately at d_m = 0.17d But, overall, the difference between the relative value of I at d_m and neighboring values is at most 5 units whereas the average value of I is around 40. This is around 12 percent. of the average value which implies that the variance for I is quite low. This is reflected in the plot

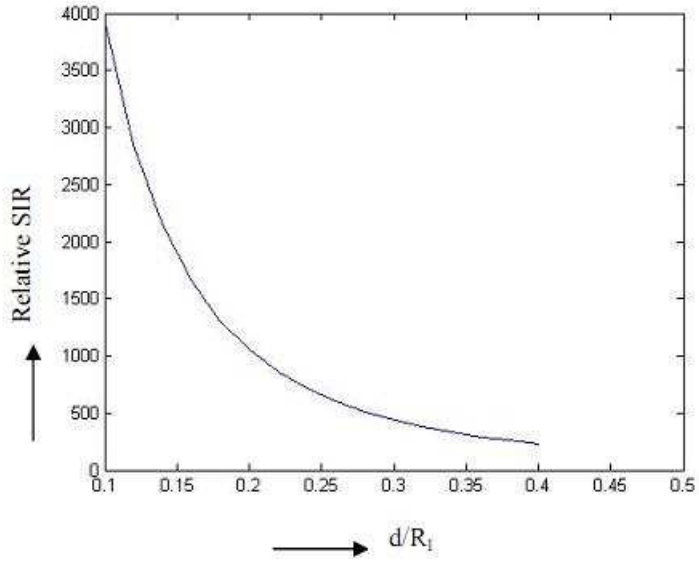

Fig.6. SIR vs d/R_I

Figure 3.5: SIR vs d/R_I

for SIR vs d/R_I where the curve is simply monotonically decreasing and the maximum at dm is not noticed.

3.3 Issues

- The 3-node analysis is incomplete as it stands as it is not yet verified whether 3-node sets contribute the most to the total SIR at Y. It might be that effective interference sets of one or two might also have a sizable contribution. Also, at best it is a crude estimate of probabilistic interference.
- As was seen with the illustration of the possibility of the existence of 4 interfering nodes, this model is geometrically quite simplified and prone to errors.
- It is not backed up by a random simulation of interference generated by random sets of nodes in the interference region. This is important as a random simulation provides the almost actual, practical data for comparison.

To address the above issues, an exhaustive and precise mathematical modeling of the situation is required, which can also be backed up by random simulation data. For this, a back-to-basics approach was adopted and the following analysis was developed.

Chapter 4

Recursive approach to non-power control

4.1 Analysis

We can express the expected value of interference in a time-slot by the following expression- $I_n = P_1 I_{11,n=1} + P_2(I_{21,n=2} + I_{22,n=2}) + P_3 I_{31,n=3}$

Where,P_I is the probability of there being total i nodes in the total shaded area .

and, $I_{ij}$is the probabilistic interference considering that only j nodes are exclusive interferers ($j \leq i$), given that there are total n nodes in the shaded region,

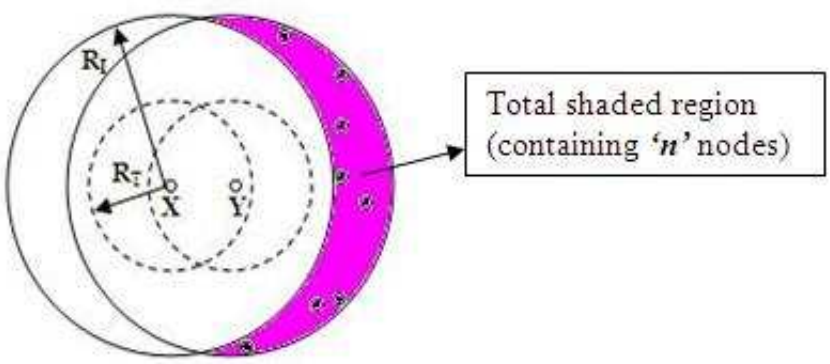

Figure 4.1: Effective Interference Area

The above formula is akin to a total conditional probability expression. It is valid for both the power control and non power control cases. It can be rewritten as -

$$\begin{aligned} I_{Total} &= (P_1 I_{11,n=1} + P_2 I_{21,n=2} + P_3 I_{31,n=3}) + (P_2 I_{22,n=2} + P_3 I_{32,n=3} + P_4 I_{42,n=4}) \\ &\quad + (P_3 I_{33,n=3} + P_4 I_{43,n=4} + P_5 I_{53,n=5}) \end{aligned} \tag{4.1}$$

$I_{Total} = Int_1 + Int_2 + Int_3 + ...$

Over here, Int_1 is the overall interference due to one effective transmitting node, Int_2 is the overall interference due to two effective transmitting nodes and so on. The expression for Int_1 was formulated as follows -

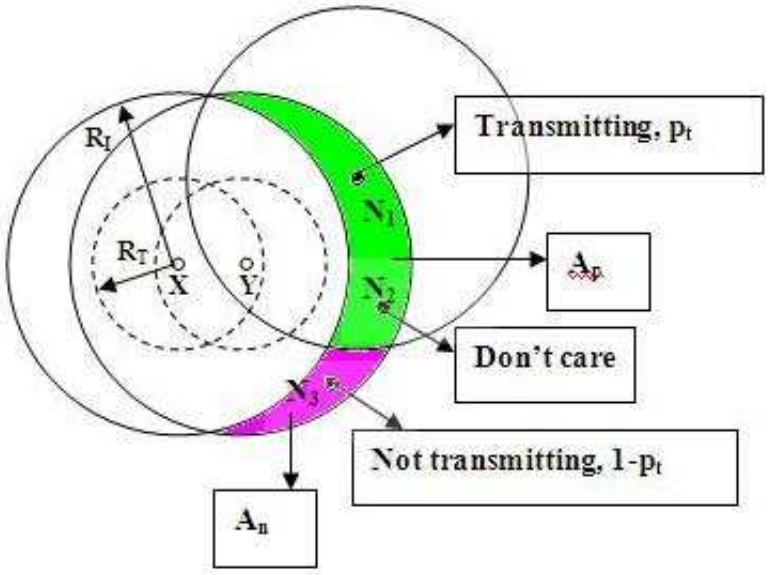

Figure 4.2: Illustration for I_{31}, when N_1 is the Interfering node

A_p (in Green) is the area common to the Interference region of N_1 and the total shaded area. A_n (in Pink) is the compliment area to A_p in the total shaded region.

In the figure above,N_1 is the only interfering (base) node and N_2 and N_3 are the other nodes in the area (which means we are considering I_{31}). N_2 falls inside the interference circle of N_1, therefore it is forced to keep quiet. Node N_3 falls outside the circle and therefore it has to be in a no-transmit mode in order to have only one node interfering overall. In a similar way, we can visualize the situation for all Int_1. Thus in this case, the expression comes out to be

$$I_{31}(A) = 1/3 \sum_{k=0}^{2} \int \int Pr(r,\alpha)_k Pr_c(r,\alpha)_{2-k} p_t (1-p_t)^2 [\frac{P_T}{r^x}] \lambda r dr d\alpha \tag{4.2}$$

By simple extension, the general expression for In_1 is :-

$$I_{n1}(A) = 1/n \sum_{k=0}^{n-1} \int \int Pr(r,\alpha)_k Pr_c(r,\alpha)_{n-k-1} p_t (1-p_t)^{n-1} [\frac{P_T}{r^x}] \lambda r dr d\alpha \tag{4.3}$$

Here, $Pr(r,\alpha)_k$ is the probability of k nodes present in the A_p region. $Pr^c(r,\alpha)_{n-k}$ is the probability of (n-k) nodes present in the A_n region. The A in the brackets after In_1 suggests that it is a function of the effective interference zone under consideration. So, the overall interference due to one effective transmitting node cases comes out to be

$Int_1 = I_{11} + I_{21} + I_{31} + ...I_{n1}....$

$$P_n = 1/n \sum_{k=0}^{n-1} \int \int Pr(r,\alpha)_k Pr_c(r,\alpha)_{n-k-1} \lambda r dr d\alpha \tag{4.4}$$

and $I_{i1/n=i}$ is actually I_{i1}/P_i thus in the overall expression P_i gets cancelled out. The (1/n)

factor with P_n and I_{n1} has been added to make them consistent with the actual expression for P_n given by Poisson's Distribution.

$$P_n = e^{-\lambda A}\lambda A^n/n!$$

A similar approach was taken for I_{n2} -

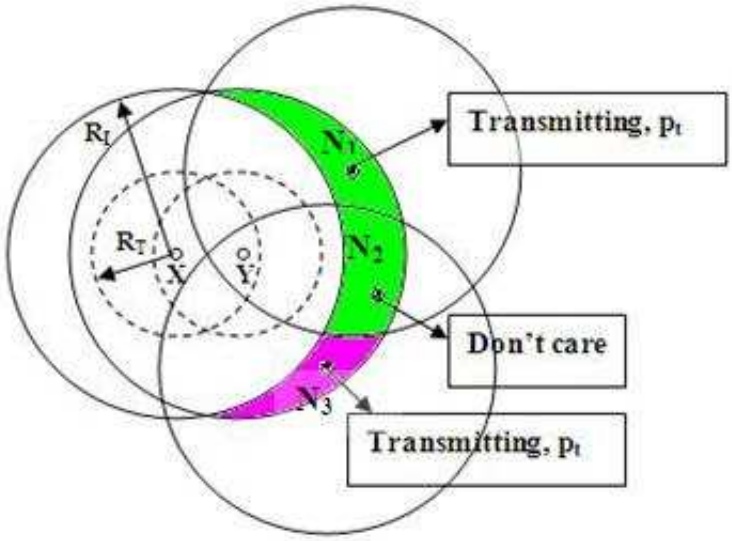

Figure 4.3: Illustration for I_{32}, when N_1 and N_3 are the Interfering nodes

The only difference here as opposed to the previous explanation for I_{n1} is that N_3 has to transmit. In general, the only condition for I_{n2} case is that there should be effectively one node transmission from A_n. If we write this out in mathematical terms, we get an expression as follows -

$$I_{22}(A) = 1/2 \int\int p_t[\frac{P_t}{r^x} + I_{11}(A_n)]\lambda r dr d\alpha \tag{4.5}$$

Here $I_{11}(A_n)$ is a function of A_n (as it geometrically exists). Similarly, the other expressions are-

$$I_{32}(A) = 1/3 \sum_{k=0}^{1} \int\int Pr(r,\alpha)_k Pr_c(r,\alpha)_{2-k} P_t[\frac{P_t}{r^x} + I_{2-k,1}(A_n)]\lambda r dr d\alpha \tag{4.6}$$

$$I_{42}(A) = 1/4 \sum_{k=0}^{2} \int\int Pr(r,\alpha)_k Pr_c(r,\alpha)_{3-k} P_t[\frac{P_t}{r^x} + I_{3-k,1}(A_n)]\lambda r dr d\alpha \tag{4.7}$$

and the General Expression is

$$I_{n2}(A) = 1/n \sum_{k=0}^{n-2} \int\int Pr(r,\alpha)_k Pr_c(r,\alpha)_{n-k-1} P_t[\frac{P_t}{r^x} + I_{n-k-1,1}(A_n)]\lambda r dr d\alpha \tag{4.8}$$

The equation above is recursive in a sense as the calculation of I_{n2} requires the computation of I_{k1} , albeit for the complement area (A_n) each time. So, the overall interference due to two effective interfering nodes comes out to be

$Int_2 = I_{22} + I_{32} + I_{42} + ...I_{n2}....$

Finally, we arrive at the three effective transmitting nodes case.

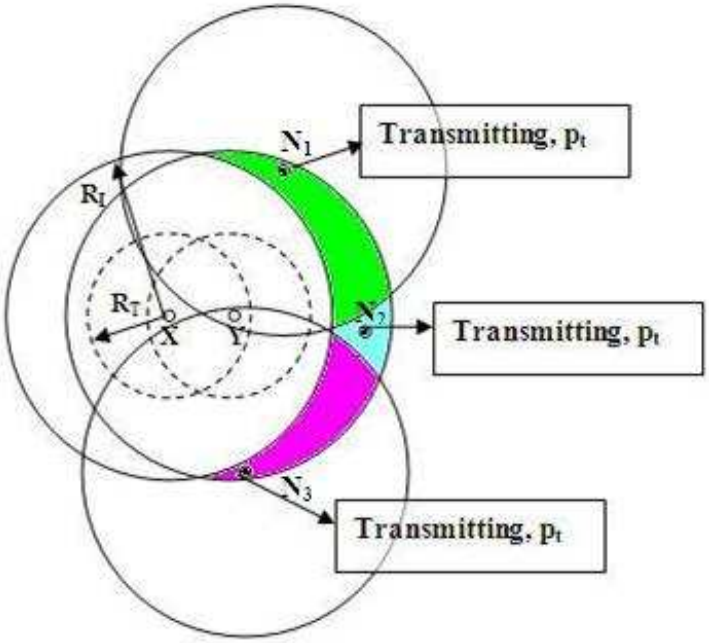

Figure 4.4: Illustration for I_{33}, when N_1, N_2 and N_3 are the Interfering nodes

As was the case with I_{n2}, the calculation of I_{n3} requires a recursive approach. The only change here is that only two nodes out of the remaining nodes in A_n are required to interfere. So for I_{33} the equation will be as follows-

$$I_{33}(A) = 1/3 \int \int Pr(r,\alpha)_k Pr_c(r,\alpha)_{2-k} P_t[\frac{P_t}{r^x} + I_{2-k,2}(A_n)]\lambda r dr d\alpha \tag{4.9}$$

So indirectly I_{33} is still an expression recursively dependent on I_{k1}, for the relevant values of k. The other expressions follow suit -

$$I_{43}(A) = 1/4 \sum_{k=0}^{1} \int \int Pr(r,\alpha)_k Pr_c(r,\alpha)_{3-k} P_t[\frac{P_t}{r^x} + I_{3-k,2}(A_n)]\lambda r dr d\alpha \tag{4.10}$$

The general expression is :-

$$I_{n3}(A) = 1/n \sum_{k=0}^{n-3} \int \int Pr(r,\alpha)_k Pr_c(r,\alpha)_{n-k-1} P_t[\frac{P_t}{r^x} + I_{n-k-1,2}(A_n)]\lambda r dr d\alpha \tag{4.11}$$

Overall the expression for the three node cases is thus -

$Int_3 = I_{33} + I_{43} + I_{53} + ...I_{n3}....$

Finally, the general result for the interference due to j nodes, when n nodes are present in the effective interference region, is

$$I_{nj}(A) = 1/n \sum_{k=0}^{n-j} \int \int Pr(r,\alpha)_k Pr_c(r,\alpha)_{n-k-1} P_t [\frac{P_t}{r^x} + I_{n-k-1,j-1}(A_n)] \lambda r dr d\alpha \quad (4.12)$$

$n \geq j$,$j \geq 2$

4.2 Results

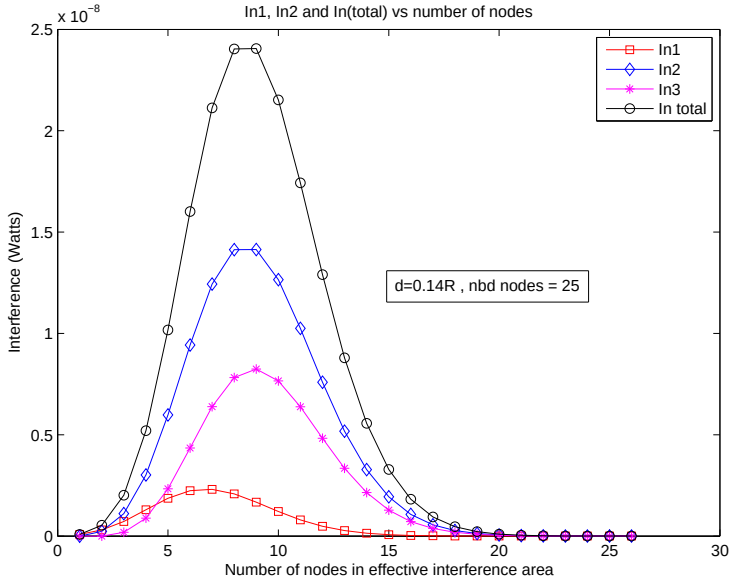

Figure 4.5: Plot for d=0.14R_I=0.28R_T and number of neighborhood nodes (within the full power transmission circle) = 25, average number of nodes in total shaded region = n_{avg} = Floor(λ A) = 8.

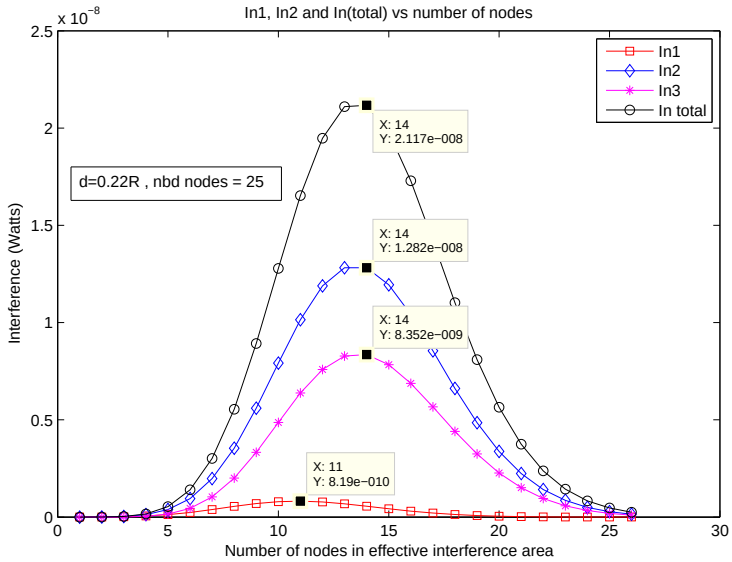

Figure 4.6: Plot for d=0.22R_I=0.44R_T, number of neighborhood nodes = 25, n_{avg}=13.

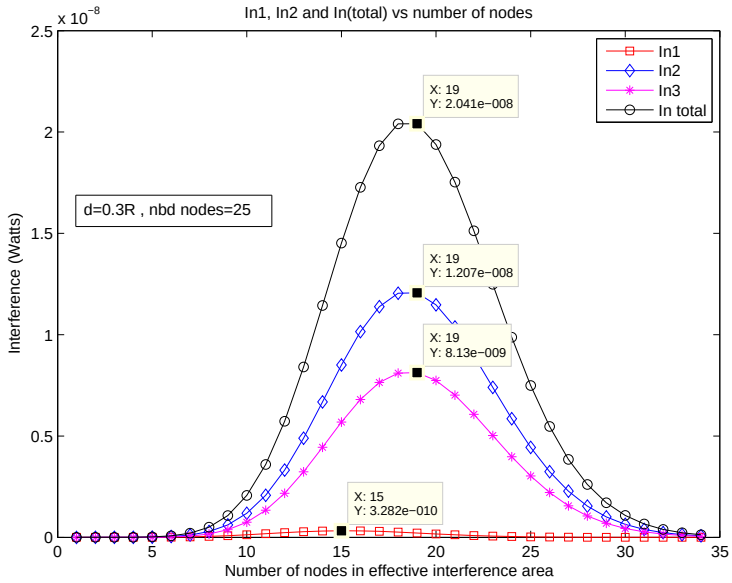

Figure 4.7: Plot for d=0.3R_I=0.6R_T and number of neighborhood nodes = 25, n_{avg}=19

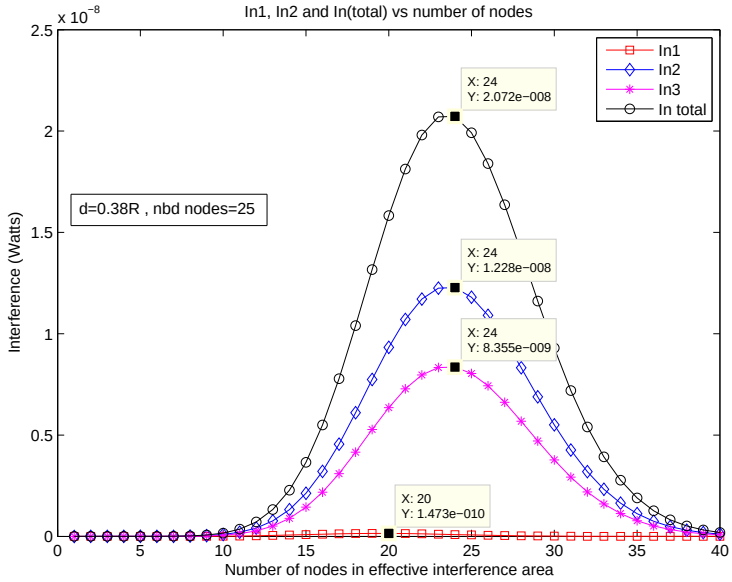

Figure 4.8: Plot for d=0.38R_I=0.76R_T and number of neighborhood nodes = 25, n_{avg}=24

4.3 Observations

- As the probability of occurrence of nodes in the region is governed by the Poisson process, the graph of the total interference peaks at the average value of the number of nodes in the effective interference region (i.e. n_{avg}) .Similarly, I_{n3} and I_{n3} also peak at the same value. On the other hand, I_{n1} shows a unique characteristic. It peaks at a value less than

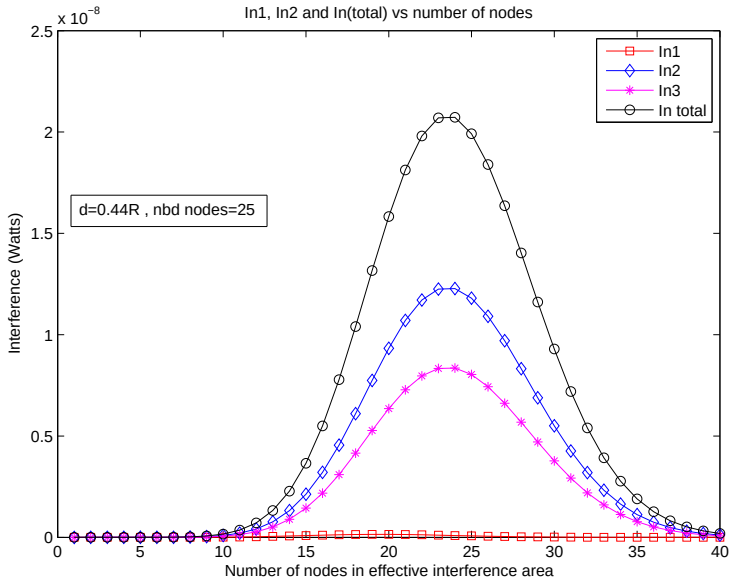

Figure 4.9: Plot for d=0.44R_I=0.88R_T and number of neighborhood nodes = 25, n_{avg}=27

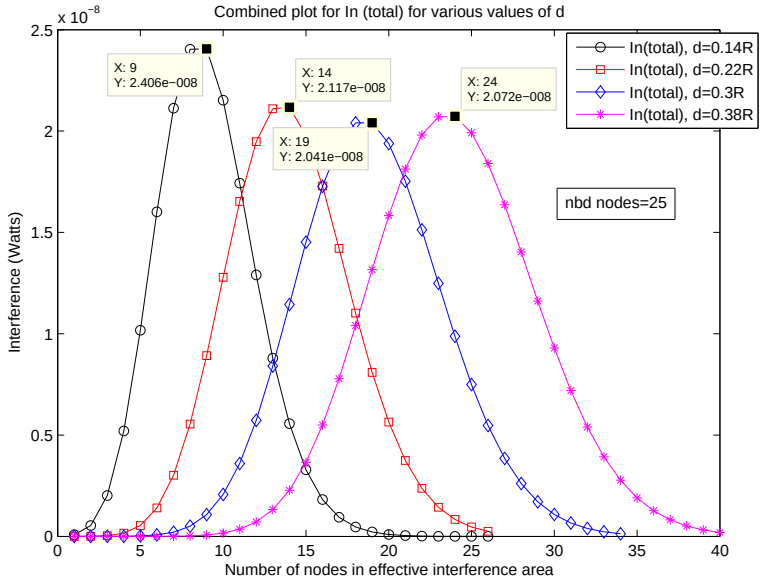

Figure 4.10: Combined plot for the above showing relative levels of $I_{n(total)}$ and I_{n2} (till d=0.38R).

n_{avg}. This is because, the no. of effective one node interference cases decreases as the total no. of nodes increase. This shifts the peak of I_{n1} slightly towards the left. But the value of In1 is quite small in relation to the values of I_{n2} and I_{n3} for any given n. Therefore, the total interference still peaks at n_{avg}.

- Also, in general, the value of I_{n2} is greater than that of I_{n3}. This is contrary to the anticipations in the 3-node method section. This is because, on a whole, the probability that three nodes interfere is lesser than that of only two nodes interfering. This relative difference of probability of occurrence is large enough that the mean value of I_{n2} is larger than the mean value of I_{n3}.
- The total interference, along with the major contributor I_{n2}, peaks at lower values as d increases. This could be because the average value of distance of the interfering nodes increases with d, thus decreasing the interference at Y.
- As seen from the combined plot, the value of maximum total interference actually increases from d=0.3R to 0.38R and then to 0.44R. This could be because at this point the effect of the increase in the area of the effective interference zone begins to override the average distance of the interfering nodes from Y.

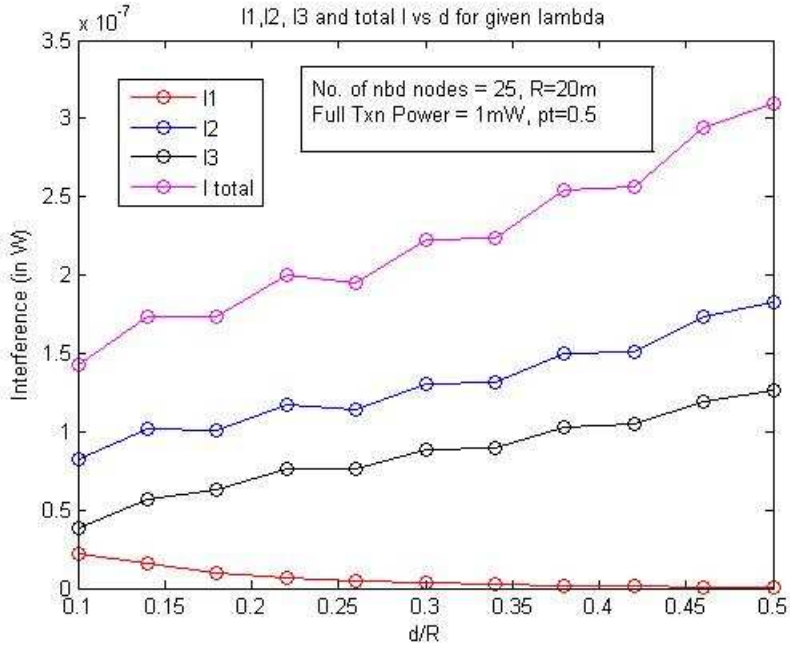

Figure 4.11: Int_1, Int_1, Int_3 and total interference comparison for various values of d

This plot is essentially the area under the I_{n1}, I_{n2}, I_{n3} and $I_{n(total)}$ curves for values of d from $0.1R_I$ ($0.2R_T$) to $0.5R_I$ (R_T). It can be seen that I (total), I_2 (=Int_2) and I_3 (=Int_3) increase in value as d increases, but I_1 (=Int_1) decreases. This can be mainly attributed to the fact that as d increases, the total number of nodes in the total shaded region (possible interferers) increases thus decreasing the probability of just one effective interfering node. Since the non-power control case is somewhat akin to MFR (with the only difference being that all values of d are equally probable in non-power control whereas there is a particular probability density function for d in MFR), one can conclude that it is better to choose the closest node for the least interference.

- The Interference value increases as the receiver moves away (i.e. d increases).

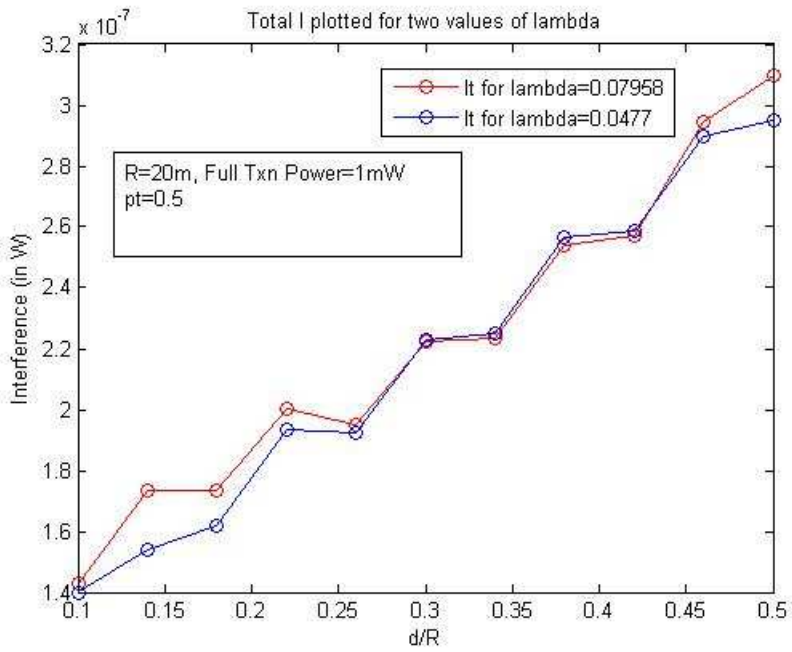

Figure 4.12: Int1, Int2, Int3 and total interference comparison for various values of d

- This can be explained by the increased number of nodes in the shaded region on an average as d is increased.
- But this graph suggests that by varying λ, we do not see a very significant change in the total interference. The value of lambda=0.07958 corresponds to 25 neighborhood nodes for transmission and that of lambda=0.0477 corresponds to 15 neighborhood nodes.

- The signal to interference ratio (SIR) decreases as d increases.
- When d is very small, the power received is large and also the interference is low. So, the SIR value is very high.
- As Interference also monotonically increases with d, the SIR curve continues to show a decrease with increasing d.

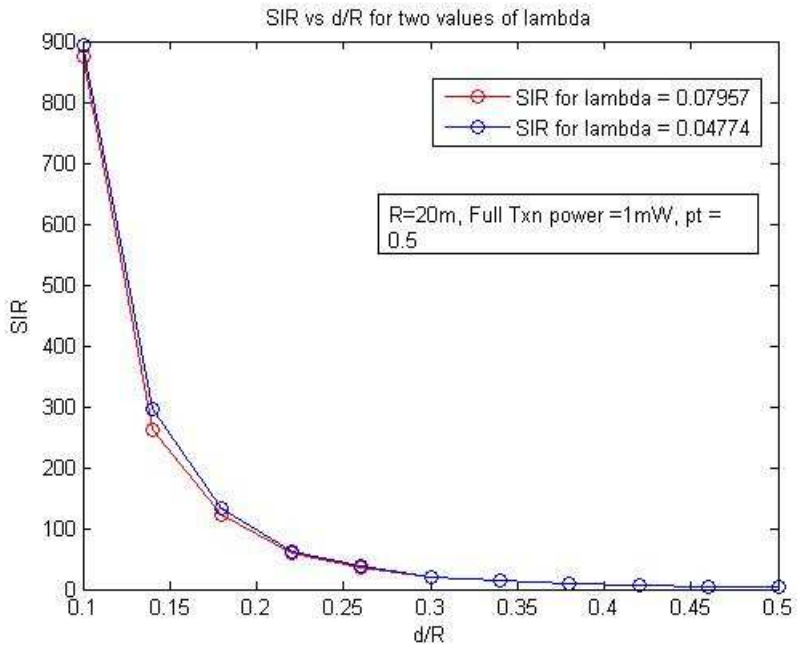

Figure 4.13: Int1, Int2, Int3 and total interference comparison for various values of d

4.4 Simulation

A 'brute-force', random simulation is needed to verify the data from the equations. The simulation has to simulate the Poisson's node distribution, the transmit/no-transmit possibility of each node in the effective interference region and the order in which they transmit (there is always some element of non-synchronization among the nodes w.r.t time-slots). The simulation algorithm developed to achieve this was-

- To simulate the Poisson distribution of nodes, a large square area (dimensions $>> R_I$) was taken and the average number of nodes (= λ*square area) were randomly positioned within it.
- A list is created of all the nodes located in the total shaded region (say n nodes) and a transmitting nodes only sub-list is randomly assigned based on probability of transmission.
- Then a random order within the transmitting nodes is selected and finally after isolating the nodes which are exclusive of each others' interference zones, the final effective interfering nodes are determined (say j nodes).
- The appropriate I_{nj} is updated and finally each of these is divided by the total number of iterations to give the actual results. The number of iterations should be quite large (minimum 10^5) to achieve stability in the results.

An alternate, slightly faster algorithm was taken before this in which the second step was simplified. According to it, suppose we have I_{n1} under consideration and there are m ($<$ n)

other nodes within the interference circle of the base node. Then the interference due to these nodes is evaluated as - $(p_t P_T / r^x) * (1 - p_t)^{n-m-1}$. This removes the randomness associated with actually assigning transmission status based on p_t. Rather, this approach takes in to account all possible sub-lists of transmitting nodes within the given list of n nodes. This is because the random method will assign txn. status to the m nodes and the sum of all possibilities=

$$\sum_{k=0}^{m} p_t^k [1 - p_t]^{m-k} = (p_t + 1 - p_t)^m = 1 \tag{4.13}$$

Therefore, this alternate method is not exactly random as is the first method, and is expected to show lesser agreement with the analysis data.

Following are some plots obtained with the first algorithm-

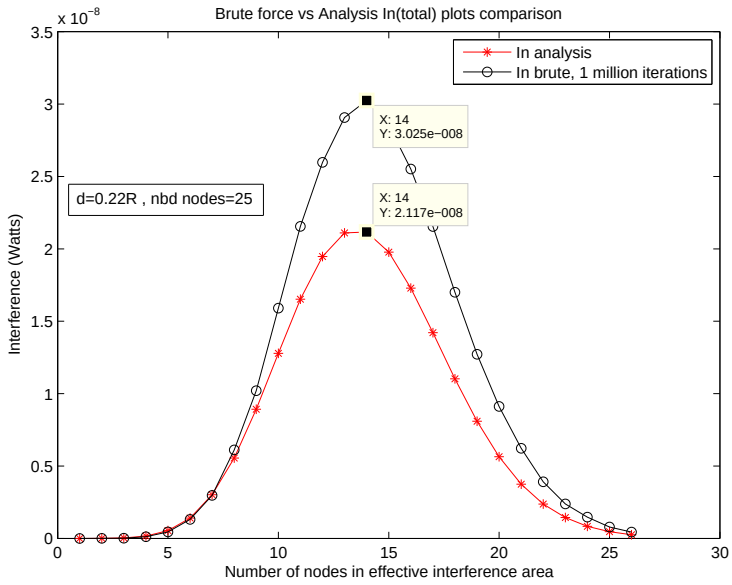

Results obtained from the simulation and the ones from the analysis showed a significant match as the number of iterations was increased. Also, importantly the shape of the curves is consistent, i.e. they peak at the same value of number of nodes (which is equal to the average node count in total shaded region).

Chapter 5

Recursive approach to Power-Controlled Tranmission

5.1 Analysis

The total interference formula remains the same in the power control case as well

$$I_n = P_1 I_{11,n=1} + P_2(I_{21,n=2} + I_{22,n=2}) + P_3 I_{31,n=3} \tag{5.1}$$

But the expressions for I_{n1}, I_{n2} etc. will have to be modified. The only difference with respect to the original equations comes in the actual interference amount. Instead of full power P_T, it will be P_T(z), where z is the current distance from the interfering node under consideration and its intended receiver. It will interfere with Y only if $z \geq r/2$, where r is its distance from Y. Obviously $z \leq R_T$. Thus the integral for I_{n1} (say) can be modified as follows-

$$\begin{aligned} I_{n1}(A) \quad &= 1/n \int_{w=R_{ff}}^{w=R_T} f_r(w) \sum_{k=0}^{n-1} \int\int \int_{z=r/2}^{z=R_T} \quad Pr(r,\alpha)_k Pr_c(r,\alpha)_{n-k-1} p_t q f_r(z) \\ &\qquad \frac{P_T(z)}{r^x} dz \lambda dr d\alpha dw \end{aligned} \tag{5.2}$$

Here R_{ff} is the distance for the node to be in the far field of the transmitter X. And

$$R_{ff} = \frac{2D^2}{\lambda} \tag{5.3}$$

where D is the maximum dimension of the larger of transmitter or receiver.

Here w stands for the variable distance between X and Y, f_r(r) is the pdf for the distance between a transmitter and receiver as given by the forwarding strategy, z is the variable for the distance between the base interferer and its receiver (in order to interfere, varies from r/2 to R_T), $P_T(z)$ is the transmission power as per the current value of z and can be given by

$$P_T(z) = \frac{P_T(R_T)}{R_T^x} z^x \tag{5.4}$$

Note that P_T (R_T) is the maximum range transmission power (same as P_T in non-power control case). The lower limit for w can be fixed by the characteristics of the forwarding

strategy, e.g. for NFP, the value of $f_r(r)$ is higher for small r and decreases with increase in r. Whereas for MVR, the value of $f_r(r)$ is increases with increases in r. Here, the q factor is of interest. Actually, we can't substitute $(1-p_t)^{n-k-1}$ over here, as it is possible that some or all of the (n-k-1) nodes in A_n transmit, but with insufficient power to cause interference at Y). It turns out that q is very complex to compute as it depends on the particular positions of the nodes in A_n, the particular distance (z) for which each of these nodes transmit (less than distance from Y/2 in order to cause no interference at Y, whether each one transmits or not at all etc. The only way to estimate q is to first carry out the brute-force random simulation for each forwarding strategy and estimate the value of q from there. Since q is different for each n (total number of nodes in the interference region), the factor was taken for the average number of nodes in the area and assumed same for all. For I_{n1}, the factor q is 1- P_r (probability that I_{nj} / j>1 occurs, given one node at least is interfering) ≈ 1-(Total number of occurrences for I_{nj} j>1 . After conducting the random simulation (described later), the factors were extracted and used.

The other expressions are-

$$I_{n2}(A) = 1/n \int_{w=R_{ff}}^{w=R_T} f_r(w) \sum_{k=0}^{n-2} \int\int\int Pr(r,\alpha)_k \; Pr_c(r,\alpha)_{n-k-1} p_t q f_r(z) [\tfrac{P_T(z)}{r^x} + I_{n-k-1,1}(A_n)] \; dz\lambda dr d\alpha dw, n \geq 2 \tag{5.5}$$

$$I_{n3}(A) = 1/n \int_{w=R_{ff}}^{w=R_T} f_r(w) \sum_{k=0}^{n-3} \int\int\int Pr(r,\alpha)_k Pr_c(r,\alpha)_{n-k-1} p_t q f_r(z) [\tfrac{P_T(z)}{r^x} + I_{n-k-1,2}(A_n)] dz\lambda dr d\alpha dw, n \geq 3 \tag{5.6}$$

And the General Expression is :-

$$I_{nj}(A) = 1/n \int_{w=R_{ff}}^{w=R_T} f_r(w) \sum_{k=0}^{n-j} \int\int\int Pr(r,\alpha)_k Pr_c(r,\alpha)_{n-k-1} p_t q f_r(z) [\tfrac{P_T(z)}{r^x} + I_{n-k-1,j-1} A_n] dz\lambda dr d\alpha dw \tag{5.7}$$

$$n \geq 3, j \leq n$$

The q factor for $I_{n-k-1,1}({}_An)$ in $I_{n2}(A)$ is 1-P_r(probability that I_{nj} (j>1) occurs, given that one node at least is interfering) ≈ 1-(Total number of occurrences for I_{nj} (j>2)/Total number of occurrences for I_{nj} ($j \geq 2$))

5.2 Plots of NFP

For the plots the value of $f_r(r)$ for NFP was changed to include the full circle and not just the forward half circle (as the direction of transmission for the interfering nodes cannot be fixed randomly). Thus the modified NFP for the analysis computation was taken as-

$$f_r(r) = \frac{2\lambda\pi r e^{-\lambda\pi r^2}}{1 - e^{-N}} \tag{5.8}$$

Where N is the average number of nodes within the transmission circle = $\lambda\pi R_T^2$

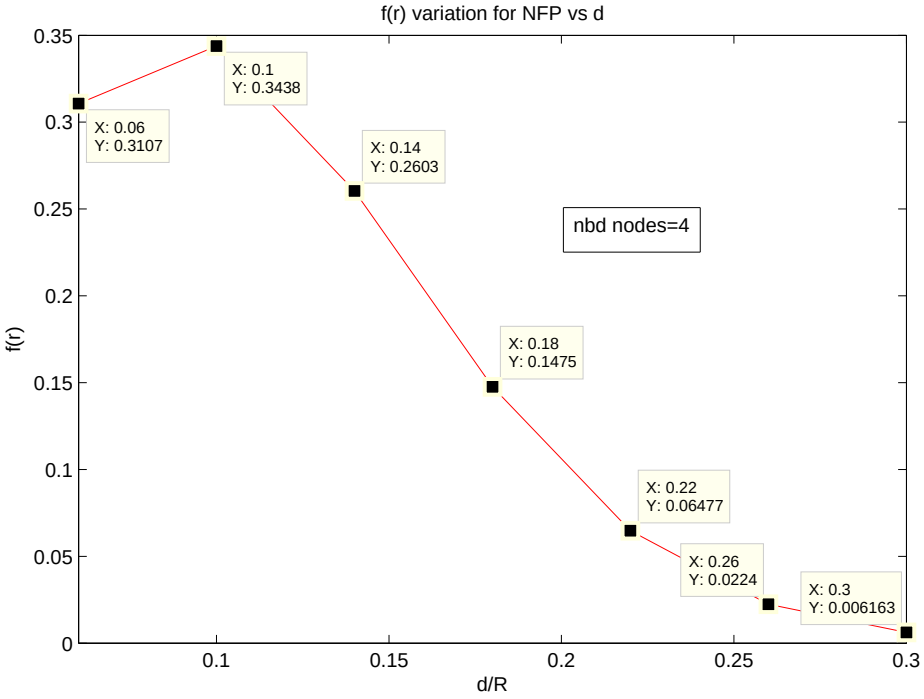

Figure 5.1: Variation of f_d with d/R_I for n_{avg}=4

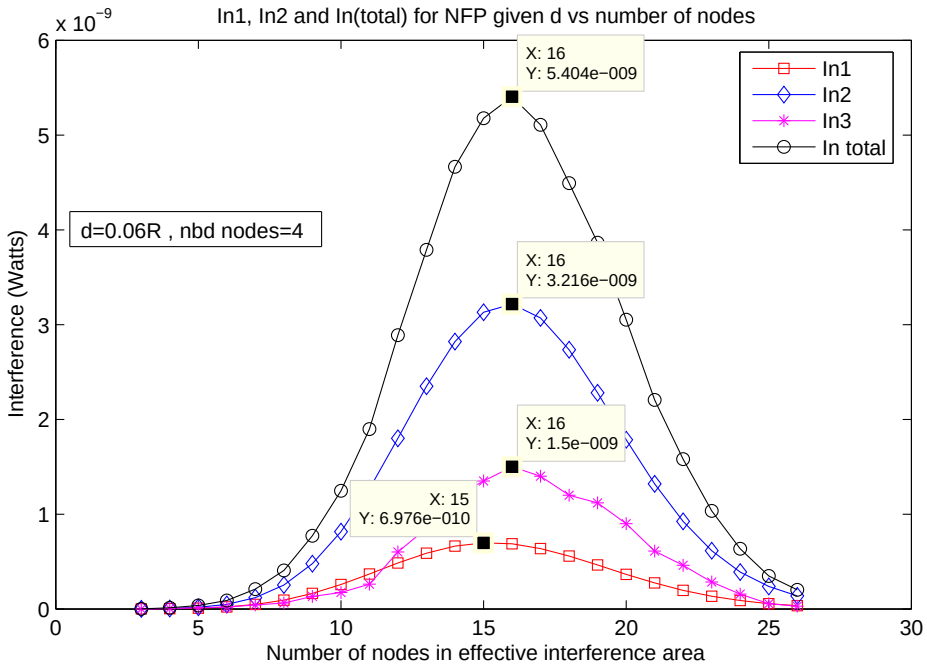

Figure 5.2: Plot for d=0.06 R_I = 0.12 R_T and number of neighborhood nodes (within the full power transmission circle) = 4, average number of nodes in total shaded region = n_{avg} = Floor(λA) = 16.

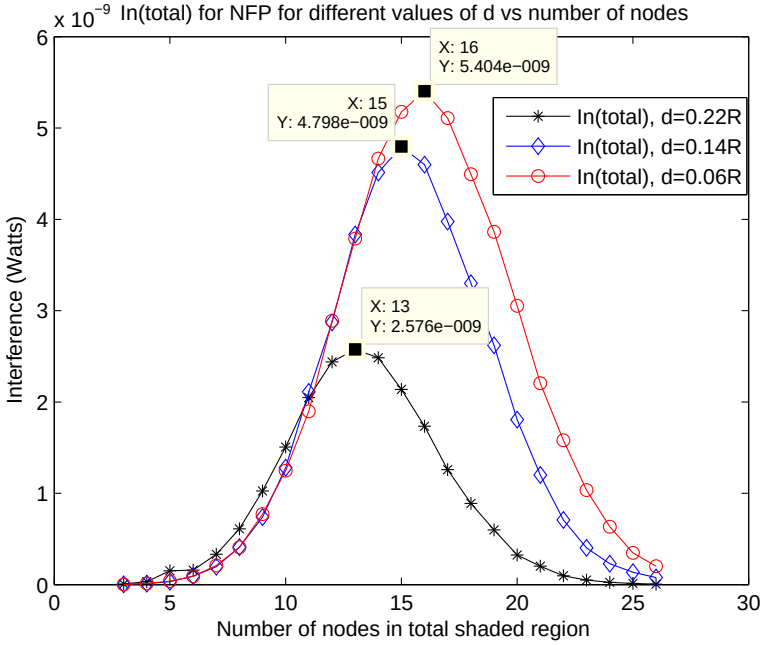

Figure 5.3: Combined Plot for In_{total} for 3 values of d

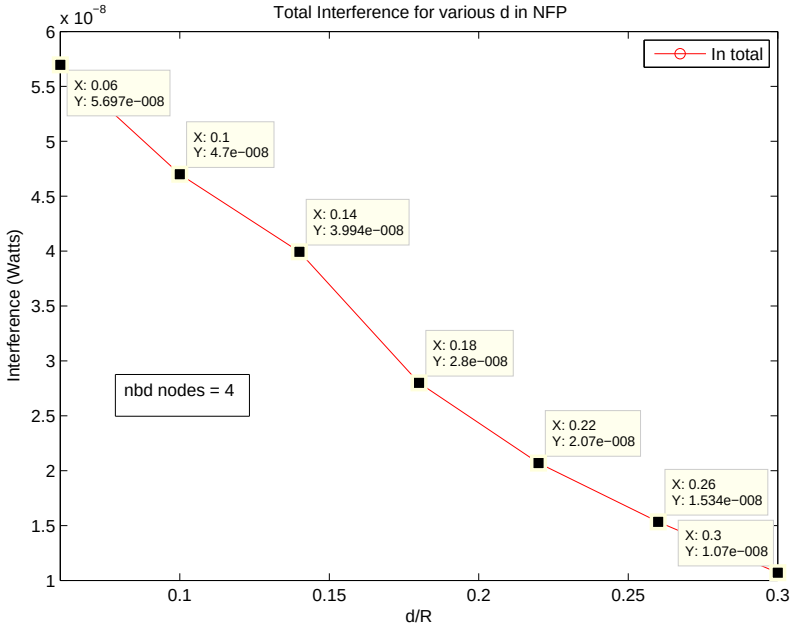

Figure 5.4: Total interference for various values of d.

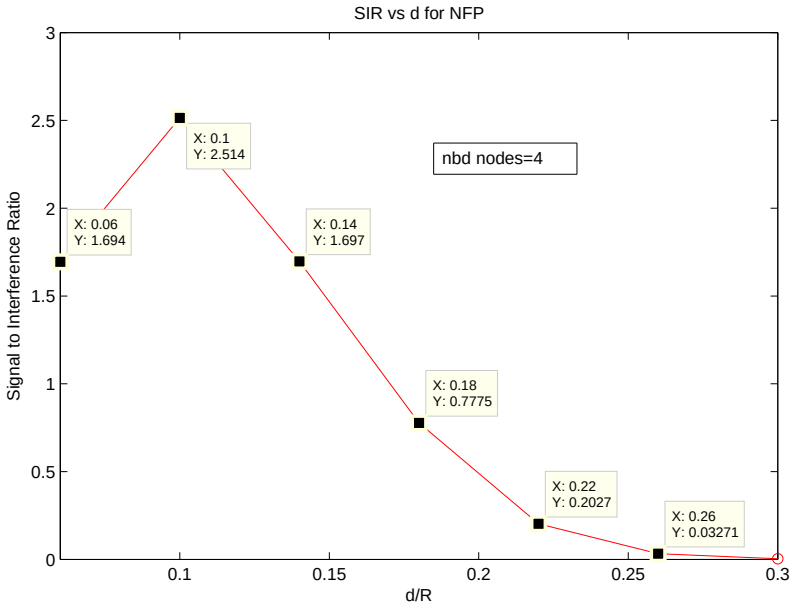

Figure 5.5: SIR for various values of d, keeping Received Power fixed.

5.2.1 Simulation

The NFP simulation algorithm is similar to the algorithm for the non-power control case. A list is made of all the values for d to be considered, for example in the case of NFP the values taken were 0.06, 0.1, 0.14, 0.18, 0.22, 0.26 and 0.3 normalized w.r.t R_I. The values for NFP have to be low as a lower value of d has a higher probability of occurrence in NFP. In the case of MVR, these values were 0.26, 0.3, 0.34, 0.38, 0.42, 0.46 and 0.49. The values have to be higher in this case as a higher value of d has a higher probability of occurrence in MVR. In NFP, for each node the closest node was chosen as the receiver and in MVR the furthest occurring node was selected. Some of the plots are as follows-

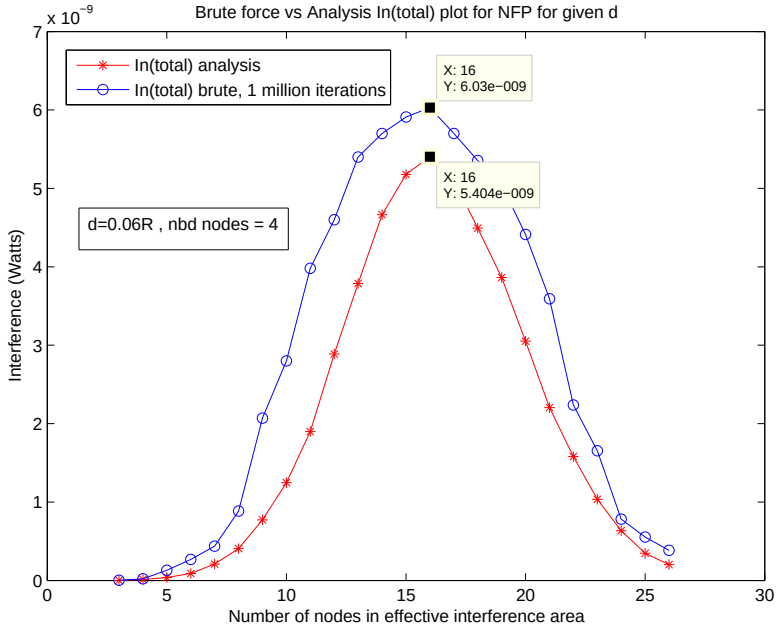

Figure 5.6: Numerical Simulation vs Analysis for NFP at d=0.06R_I and n_{avg}=4

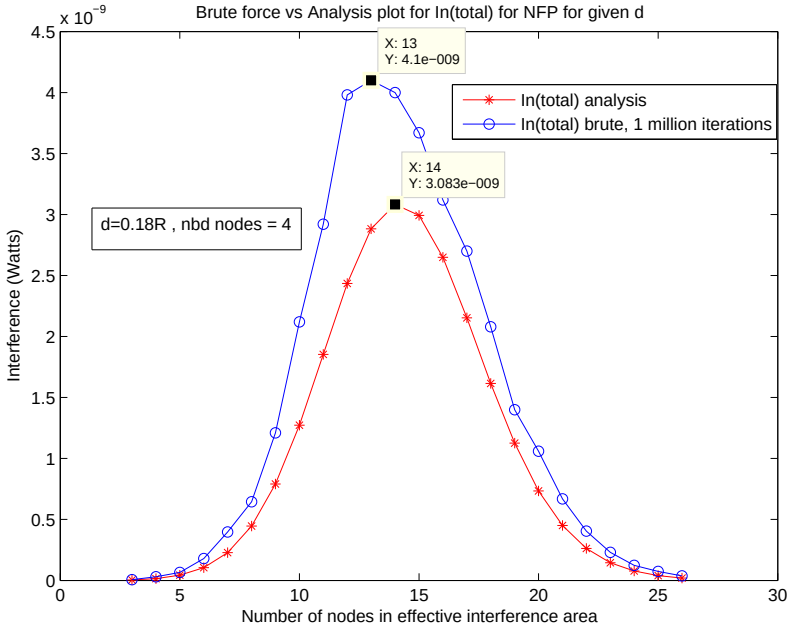

Figure 5.7: Numerical Simulation vs Analysis for NFP at d=0.18R_I and n_{avg}=4

Again, it can be seen that the brute force results closely approximate the analysis results. The value of lambda has been taken smaller than usual for both the analysis and brute force sections because the interfering area is larger in general for power-control and that increases greatly with the average number of interfering nodes(i.e. large value of λ), which greatly increased the complexity of our numerical simulation

5.2.2 Calculation of Transmitted Power and Device Power

Another important parameter to evaluate is the transmit power/device power (of a transmitting node) utilized per unit distance (d) between the one-hop transmitter and receiver. For this, the expected number of retransmissions has to be incorporated for a given expected interference. To do this, the expected BER has to be known, which requires the relationship between SINR and BER for the network under consideration. We refer here to a paper titled, **Bit Error Rate Estimation for a Joint Detection Receiver in the Downlink of UMTS/TDD** by Kopsa, Matz et al [4] which has estimated the SINR vs BER curve for a UMTS/TDD (Universal Mobile Telecommunications System/Time Division Duplex) network. This is a reasonable approximation for our network protocol as it uses QPSK modulation scheme with a W-CDMA air interface, which can be as easily a feature of a CSMA based Slotted Aloha network as well. The only difference is that UMTS/TDD uses separate downlink and uplink frequencies and time slots, which is usually not the feature with ad-hoc networks. Also the different uplink and downlink frequencies have minimal effect on power calculations.

We utilize the results obtained for a MMSE (Minimum Mean Squared Error) detector as follows-

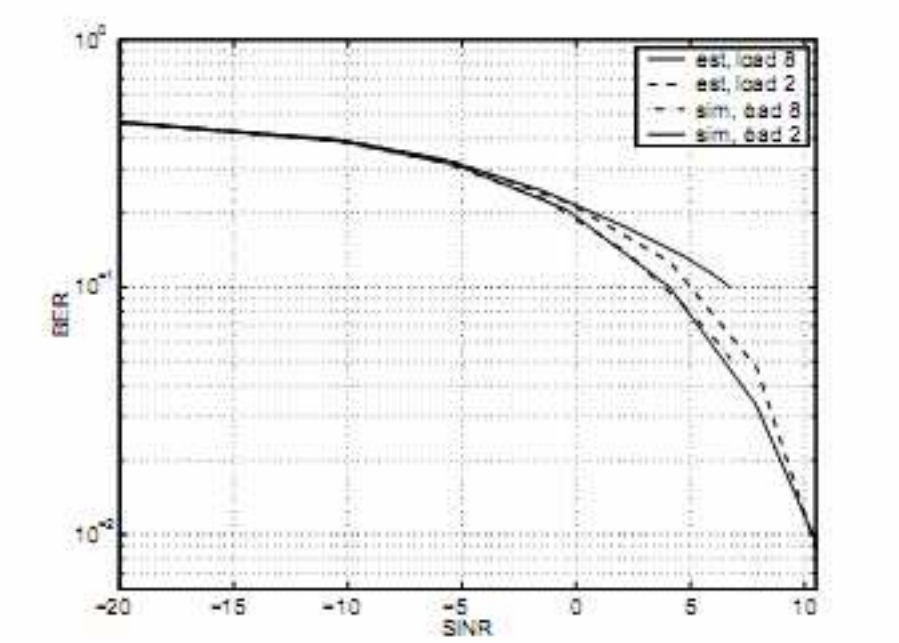

Figure 5.8: BER vs SINR curve for different values of load in the network

The load factor in this paper is the number of users in a cell, which has a radius of 30m. We have taken the average number of nodes within a transmission radius of 10m to be 4. This translates to 12 nodes within a radius of 30m. So, we use the curve given for the higher load factor i.e. 8 throughout. For each value of d, the SINR value was calculated using the expected interference value calculated, a noise level of -70 dBm (usually the indoor noise level varies from -60 dBm to -80 dBm) and the signal power at the receiver (which is constant for any power control strategy). From this value of SINR, the BER (=p_r) was estimated from the curve. Then, considering an average packet length of 8 bits, the probability of success at the decoder is

$(1-pr)^{8}$ =p_s). Assuming that there is no limit to the number of retransmissions, the expected number of retransmissions is given by 1/p_s.

Thus, the expected transmission power per unit distance is

$$E(d) = \frac{f_r(d)P_T(d)retr(d)}{d}, where P_T(d) = P_T(R)d/R^x \tag{5.9}$$

Here, $P_T(R)$ is the full range transmission power, x is the path loss factor and retr(d) is the expected number of retransmissions given d.

Another parameter of interest is the actual device power utilized for a given transmission power. For this, we use the operating specifications of the CC2420 RF transceivers manufactured by Chipcon (ref. [5])). They are as follows-

Current Consumption, transmit mode:					
P = -25 dBm		8.5		mA	The output power is delivered differentially to a 50 Ω singled ended load through a balun, see also page 53.
P = -15 dBm		9.9		mA	
P = -10 dBm		11		mA	
P = −5 dBm		14		mA	
P = 0 dBm		17.4		mA	

Figure 5.9: Transmitted Power and Current Table for CC2420 Tranceiver

For our purposes, we assume that the load resistor is 1 ohm. For each $P_T(d)$ we calculate the value of current which flows through the load (I_L) and calculate the device power used up = I_L^2 . Finally the device power utilized per unit distance is

$$Pw(d) = \frac{f_r(d)I_L^2(d)retr(d)}{d}. \tag{5.10}$$

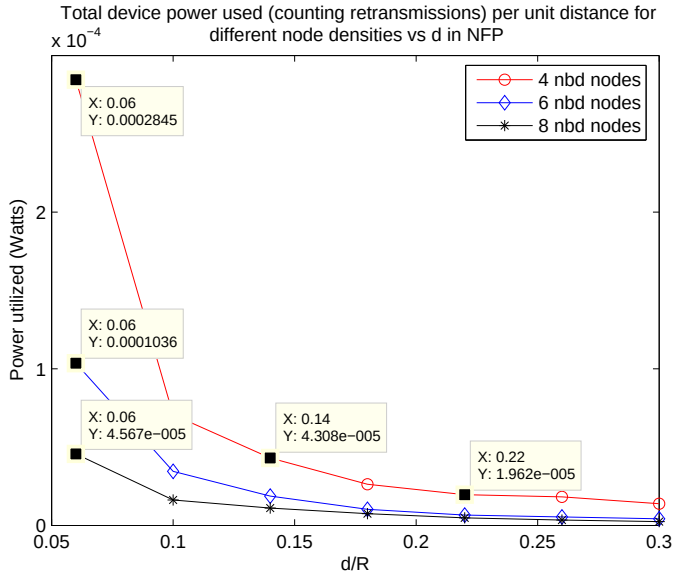

Figure 5.10: System Energy utilized per unit forward progress vs. d/R_I, for N_{avg} = 4,6 and 8

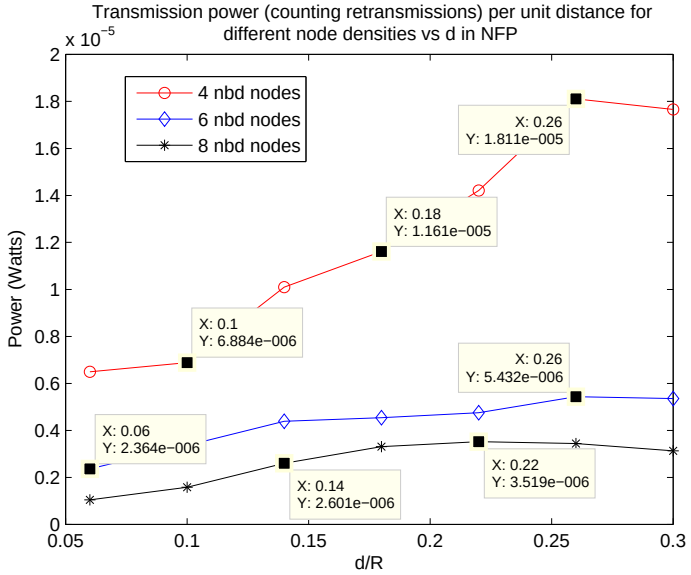

Figure 5.11: Transmitted power per unit forward progress vs. d/R_I, for N_{avg} = 4,6 and 8

5.2.3 Observations and Inferences from NFP Plot

- Acc to Fig 5.1, f_d values is a decreasing function of r
- Acc to Fig 5.2 and 5.3 interference value peaks at the value of no. of nodes in the effective interference region which is very close to N_{avg}.
- Acc to Fig 5.4 ,the total interference decreases as we choose the receiver farther in NFP transmission strategy. This may be because as d increases, the distance between the possible interfering nodes and Y increases, decreasing the probabilistic interference. One more reason for this can be the decrease of total no. of average nodes in the Effective Interference Region.
- Acc to Fig 5.5, We observe the SIR to exhibit a peak of maxima at d = $0.2R_T$ (approx).
- According to Fig 5.6 and 5.7, Brute Force Simulation and the Analysis Results are very close to each other.
- The total interference, which is given by

$$\sum_{0.12R_T}^{0.6R_T} I_n(d)\Delta d$$

  Where, Δ d = $0.08R_T$, N_{avg} = 4 is $1.7492 * 10^{-7}$ and for N_{avg} = 6 is $7.9998 * 10^{-8}$, N_{avg} = 8 is $4.7188 * 10^{-8}$ i.e. , the total interference would increase for increasing λ, as higher λ would cause the average distance between X and Y to go down thus increasing interference (as is clear from fig 5.4).
- From Fig 5.10 and 5.12, the total Device power for N_{avg} = 4 is $6.8052 * 10^{-5}$, N_{avg} = 6 is $2.4156 * 10^{-5}$ and for N_{avg} = 8 is $104899 * 10^{-5}$. Thus we can conclude that, in this range of λ, the Device power per unit d, decreases for increasing λ.
- From Fig 5.11 and 5.11, the total Transmitted power for N_{avg} = 4 is $3.8098 * 10^{-4}$, N_{avg} = 6 is $1.4663 * 10^{-4}$ and for N_{avg} = 8 is $7.3003 * 10^{-5}$ Watts. Thus we can conclude that, in this range of λ, the Transmission power required per unit d, also decreases for increasing λ.

5.3 Plots for MVR

As was with NFP, the modified expression for f(r) in MVR for the analysis computation was taken as-

$$f_{r,\theta}(r_0,\theta_0) = \frac{2\lambda r_0 e^{-2\lambda A_Z}}{1-e^{-N}}, \qquad 0 \le r_0 \le R, 0 \le \theta_0 \le 2\pi \tag{5.11}$$

where,

$$A_Z = R^2(cos^{-1}[(r_0/R)cos(\theta_0)] - (r_0/R)cos(\theta_0)\sqrt{1-[r_0 cos\theta_0/R]^2}) \tag{5.12}$$

and ,

$$f_r(r_0) = \int_{\theta=0}^{\theta=2\pi} f_{r,\theta}(r_0,\theta_0)d\theta \tag{5.13}$$

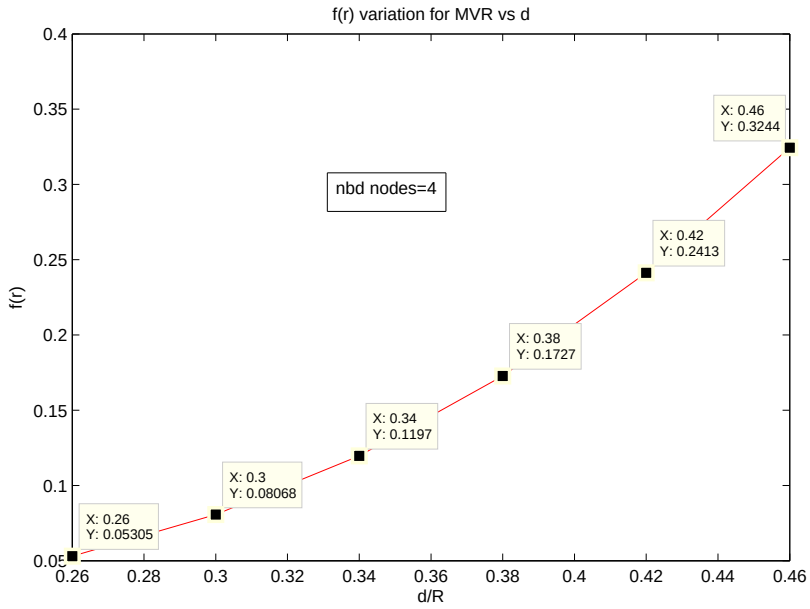

Figure 5.12: Variation of f_d with d/R_I for n_{avg}=4

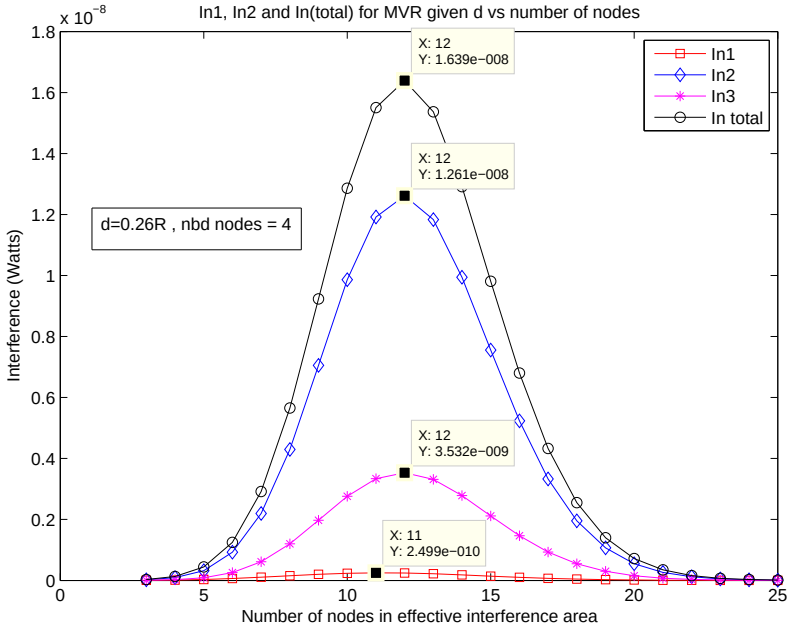

Figure 5.13: Plot for d=0.26 R_I=0.52 R_I and number of neighborhood nodes = 4, n_{avg} = 11 .

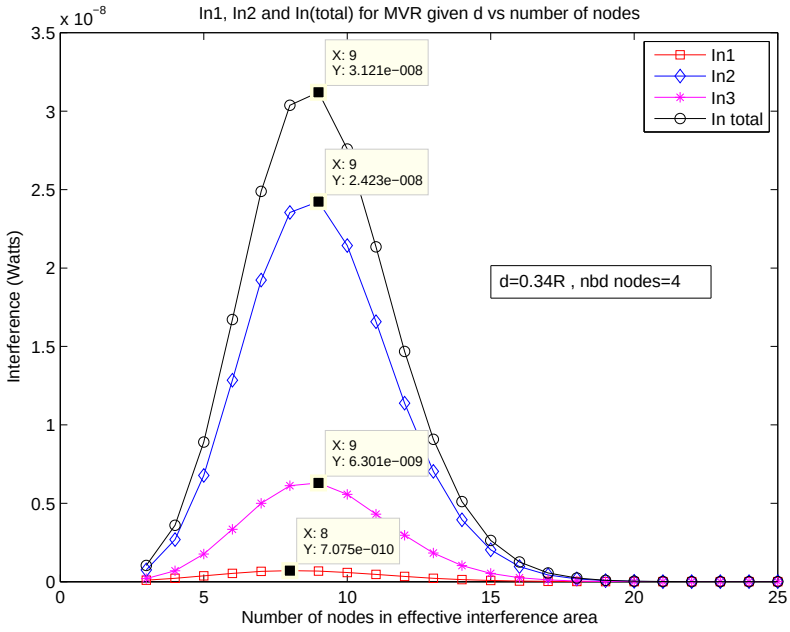

Figure 5.14: Plot for d=0.34 R_I=0.68 R_I and number of neighborhood nodes = 4, n_{avg} = 10 .

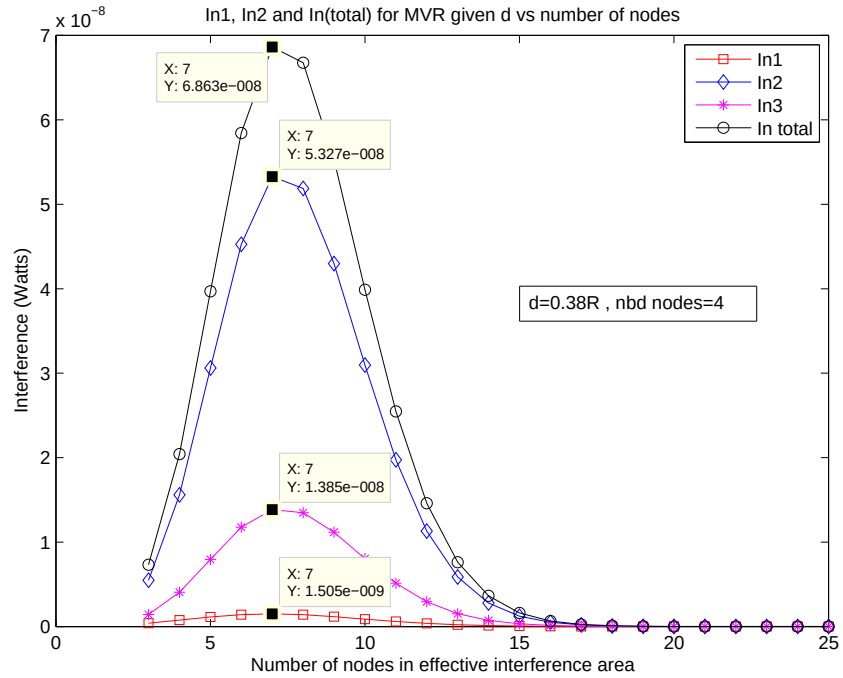

Figure 5.15: Plot for d=0.38 R_I=0.72 R_I and number of neighborhood nodes = 4, n_{avg} = 6 .

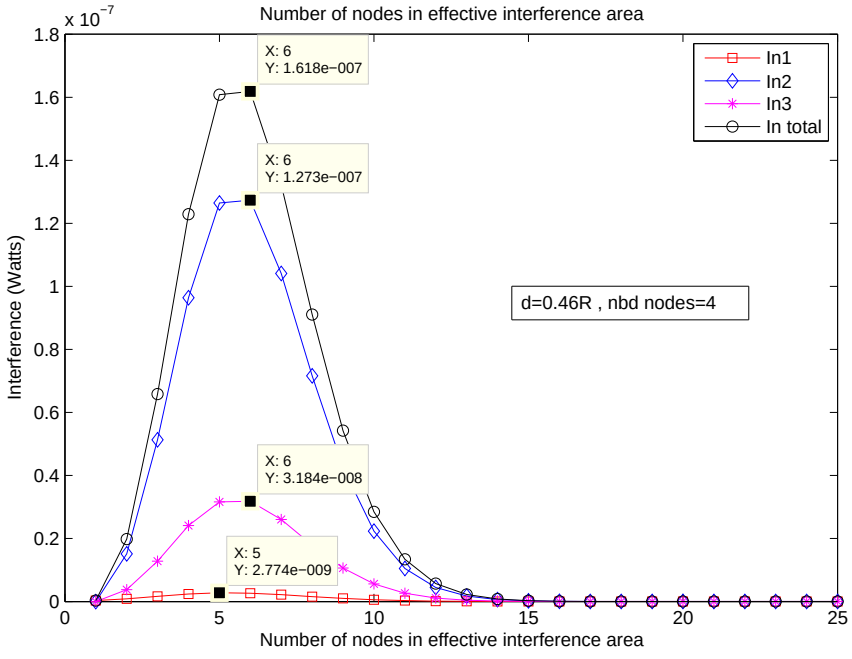

Figure 5.16: Plot for d=0.46 R_I=0.92 R_I and number of neighborhood nodes = 4, n_{avg} = 5 .

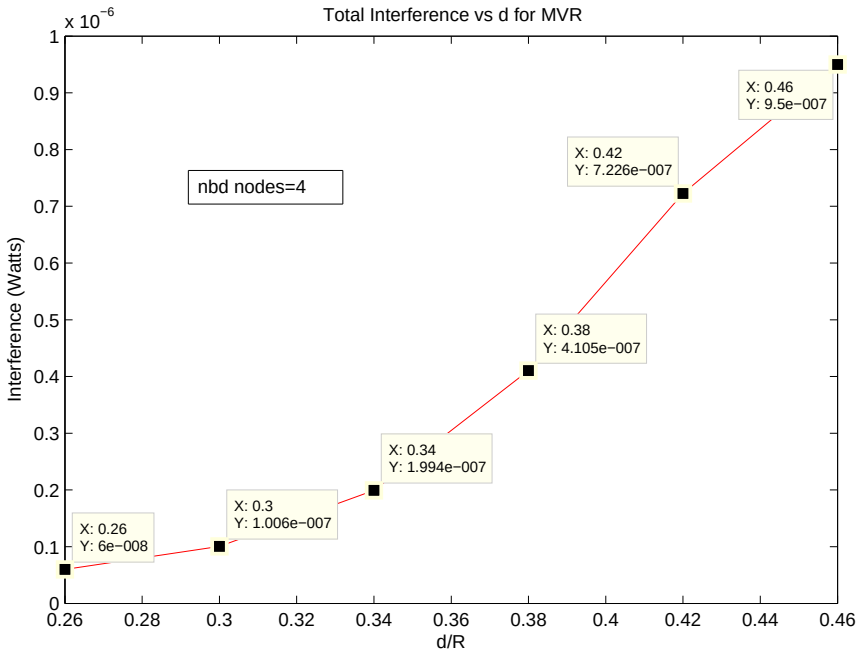

Figure 5.17: Total interference for various values of d.

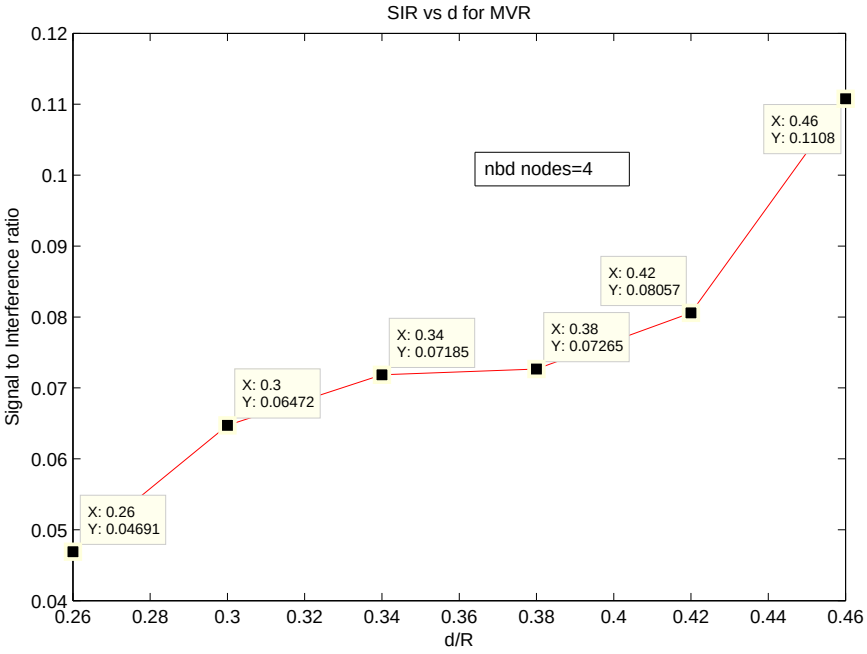

Figure 5.18: SIR for various values of d, keeping Received Power fixed.

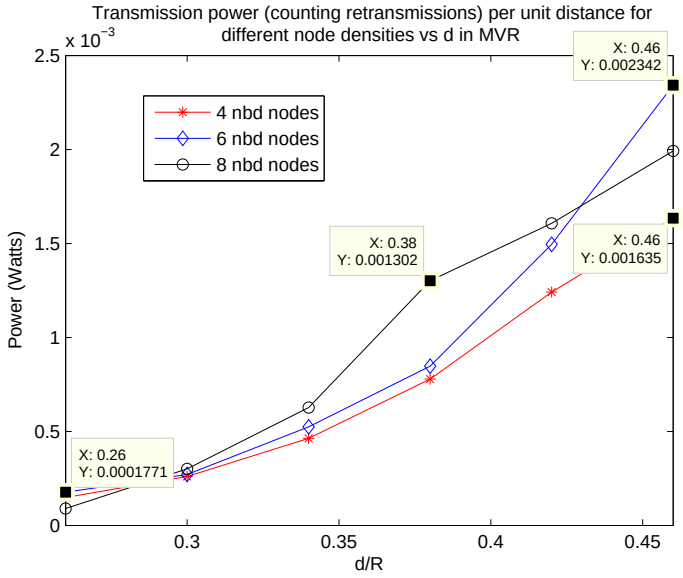

Figure 5.19: Transmitted power per unit forward progress vs. d/R_I

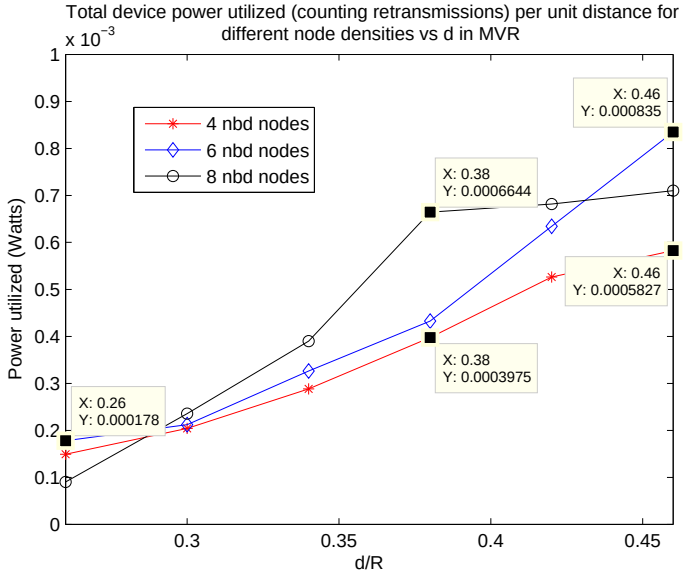

Figure 5.20: System Energy utilized per unit forward progress vs. d/R_I

The total interference for MVR, when the average number of transmission zone neighbors is 4, is $1.9544 * 10^{-006}$ **Watts or -27.09 dBm, which is greater than that for NFP.**

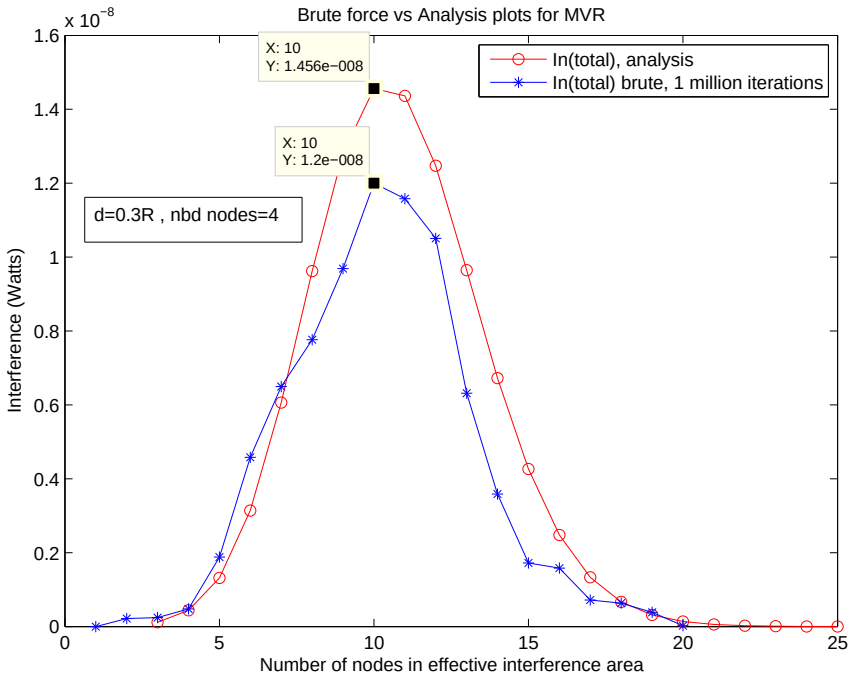

Figure 5.21: Brute Force vs Analysis Result for MVR

5.3.1 Observations and Inferences from MVR Plots

- According to Fig 5.14, f_d for MVR is a montonically increasing function of d
- According to Fig 5.19, the total probabilistic interference is a montonically increasing function of d. This is due to the increasing f_d which predominates over actual Interference values i.e. I/f_d .
- According to Fig 5.20, SIR is a montonically increasing function of d too.
- According to Fig 5.21, Transmitted Power per unit forward progress is a montonically increasing function of d. T_{Xn} Power is $P_{Recieved}d^3$ f_d/d. This explains the approx. quadratic behavior of the plot.
- For Fig. 5.22 Device Current is monotonically increasing acc to table in Fig 5.9.Thus, the device power which is proportional to I^2 increases with the increase in Transmission power, which is in turn caused due to increasing d.
- According to Fig 5.23, We can observe that the Brute Force Simulation and the Analysis Results are very close to each other.
- From Fig. 5.21, the total Transmission Power utilized per unit d,for N_{avg} = 4 is 0.0036, N_{avg} = 6 is 0.0045 and for N_{avg} = 8 is 0.0047.

- From Fig. 5.22, the total Device Energy utilized per unit d,for N_{avg} = 4 is 0.0017, N_{avg} = 6 is 0.0021 and for N_{avg} = 8 is 0.0022

5.4 Plots of Random Selection Analysis

In random forwarding, a transmitter node can select any available node and transmit data to it with power control. Thus the computational overload of selecting the appropriate receiver node like the other strategies is avoided. The $f_r(r)$ for this strategy can be given by

$$F_r(r) = \frac{r^2(1 - e^{-\lambda\pi r^2})}{R_2(1 - e^{-\lambda\pi R^2})} \tag{5.14}$$

Therefore,

$$f_r(r) = \frac{2r(1 - e^{-\pi r^2})(1 - \pi r^2)}{R^2(1 - e^{-\lambda\pi R_2})} \tag{5.15}$$

The Interference equations remain the same as before, with $f_r(r)$ given by the above equation. The q factor was estimated from the brute force simulation in which the selection policy was to select any existing node at a distance lesser than the transmission radius. The results were as follows

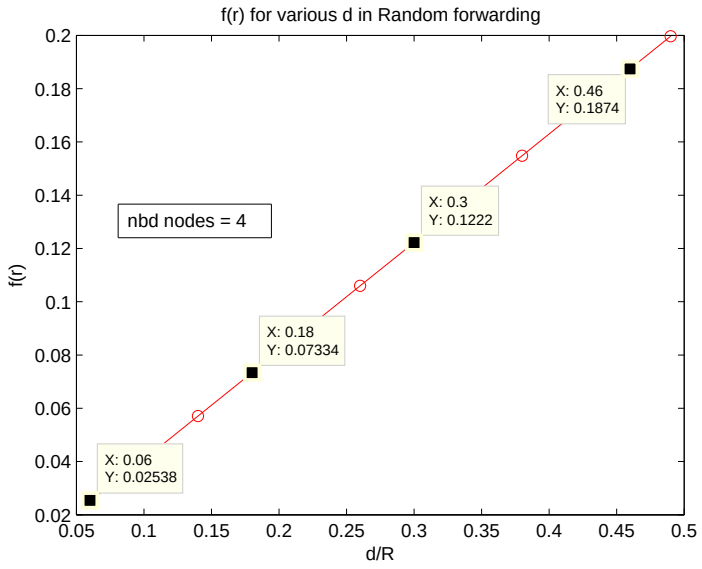

Figure 5.22: Variation of f_d with d/R_I for n_{avg}=4

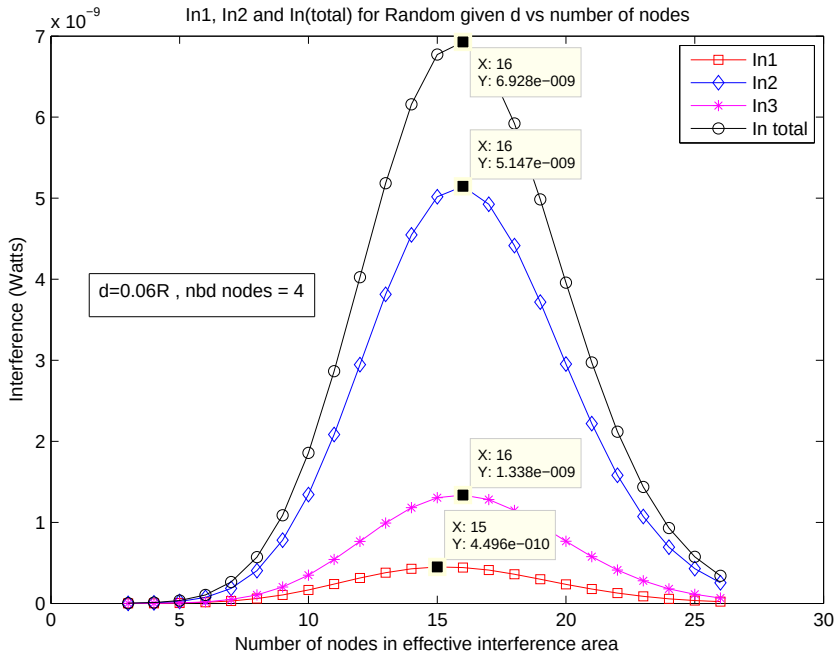

Figure 5.23: Plot for d=0.06 R_I and number of neighborhood nodes = 4, n_{avg} = 15

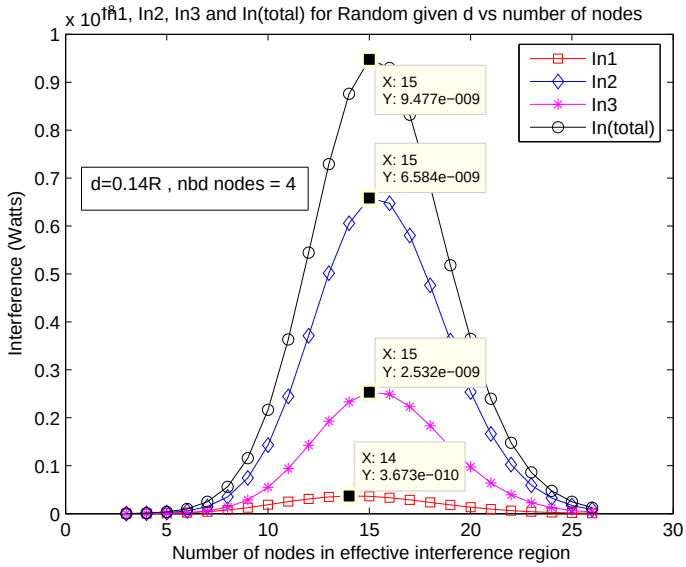

Figure 5.24: Plot for d=0.14 R_I and number of neighborhood nodes = 4, n_{avg} = 14

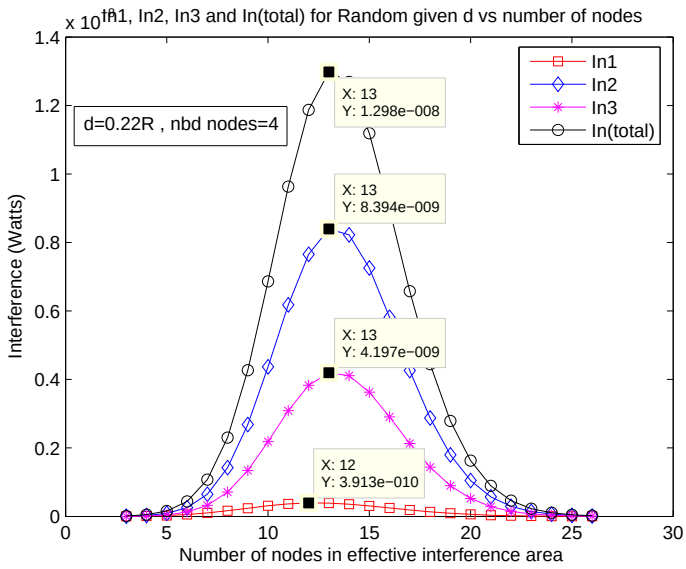

Figure 5.25: Plot for d=0.22 R_I and number of neighborhood nodes = 4, n_{avg} = 12

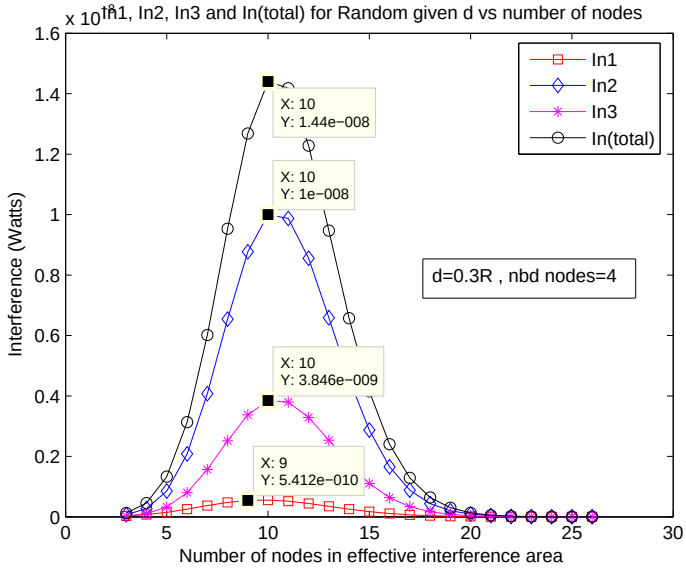

Figure 5.26: Plot for d=0.3 R_I and number of neighborhood nodes = 4, n_{avg} = 10

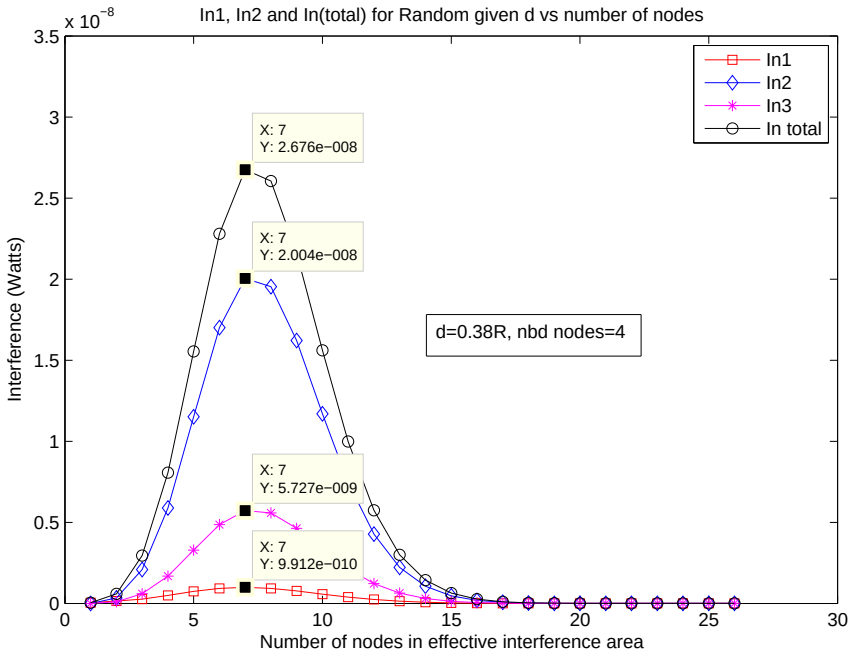

Figure 5.27: Plot for d=0.38 R_I and number of neighborhood nodes = 4, n_{avg} = 7

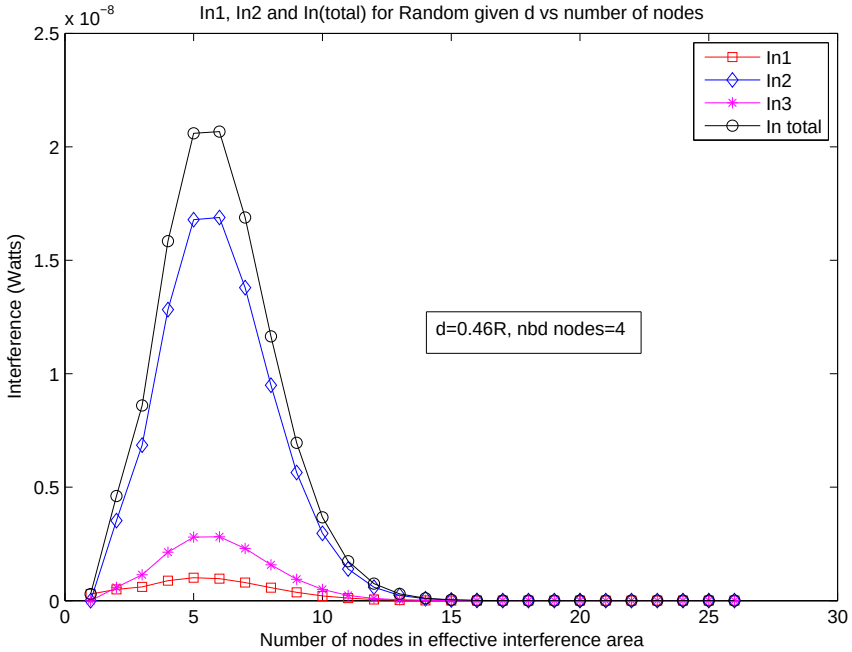

Figure 5.28: Plot for d=0.46 R_I and number of neighborhood nodes = 4, n_{avg} = 5

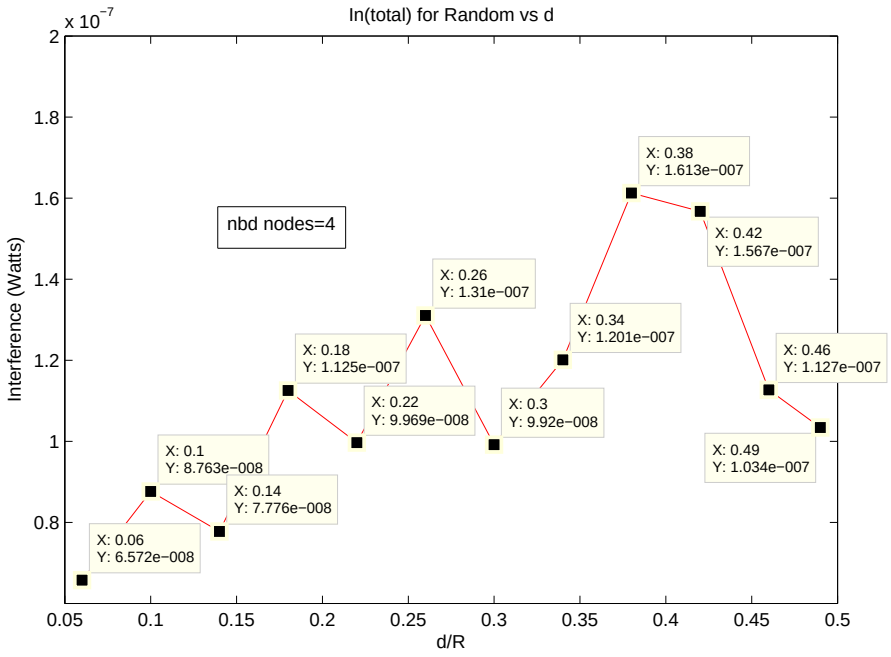

Figure 5.29: Total Interference for various values of d for random forwarding

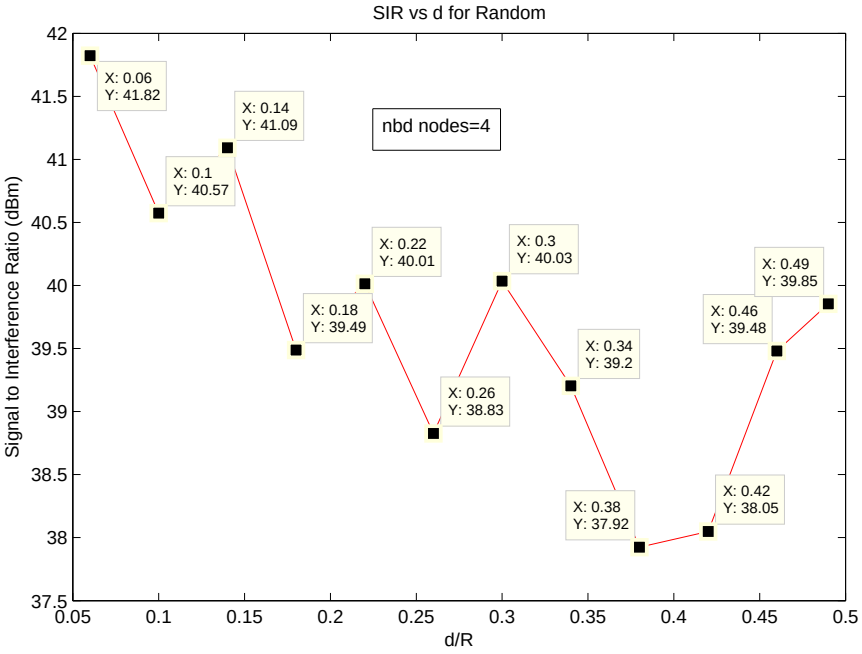

Figure 5.30: SIR vs d/R_I

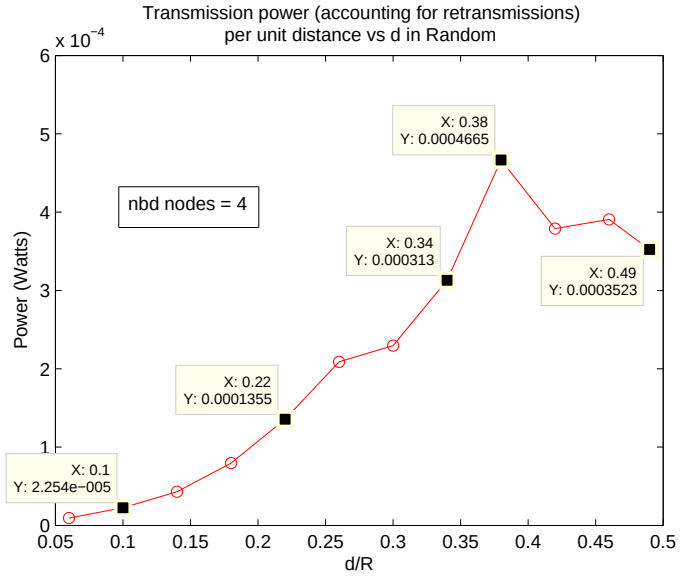

Figure 5.31: Transmitted power per unit forward progress vs. d/R_I

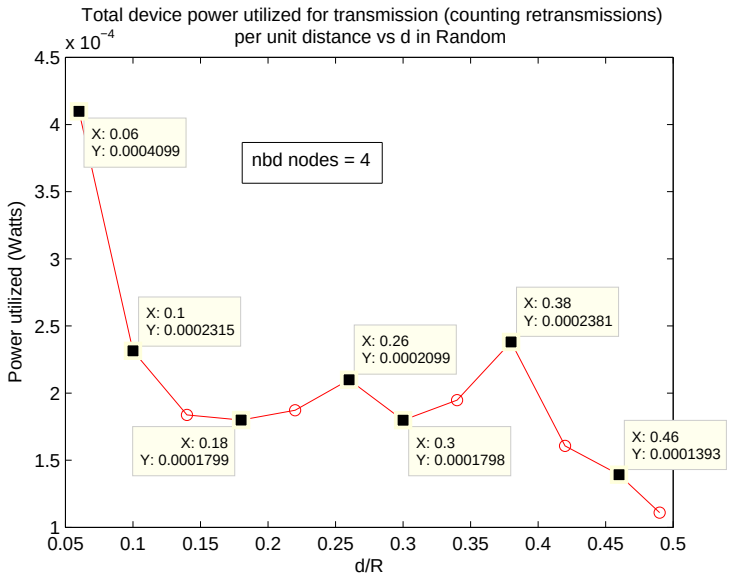

Figure 5.32: System Energy utilized per unit forward progress vs. d/R_I

5.4.1 Observations and Inferences from Random Selection Plots

- According to Fig 5.24, f_d for Random Selection is a approx linearly increasing function of d
- According to Fig 5.31, the total interference is a haphazard function of d. This can be attributed to the fact that f(r) is not a steep curve (as is the case in MVR and NFP), thus the variation is not non-monotonic.

- According to Fig 5.32, SIR shows a bit inconsistency. It keeps on increasing and decreasing.
- According to Fig 5.33, Transmitted Power per unit forward progress shows a general increment with increasing d.
- As per fig 5.34 Device Current is shows a general increase with d. Thus, the device power which is proportional to I^2 increases with the increase in Transmission power, which is in turn caused due to increasing d.
- The total Transmission Power utilized per unit d, for N_{avg} = 4 is 0.0021.
- The total Device Energy utilized per unit d, for N_{avg} = 4 is 0.0019.
- The total interference for Random Selection Strategy , when the average number of transmission zone neighbors is 4, is $1.0622 * 10^{-6}$ Watts or -29.7377 dBm, which is slightly lesser than that of MVR and more than NFP.

5.5 Critical Value of λ

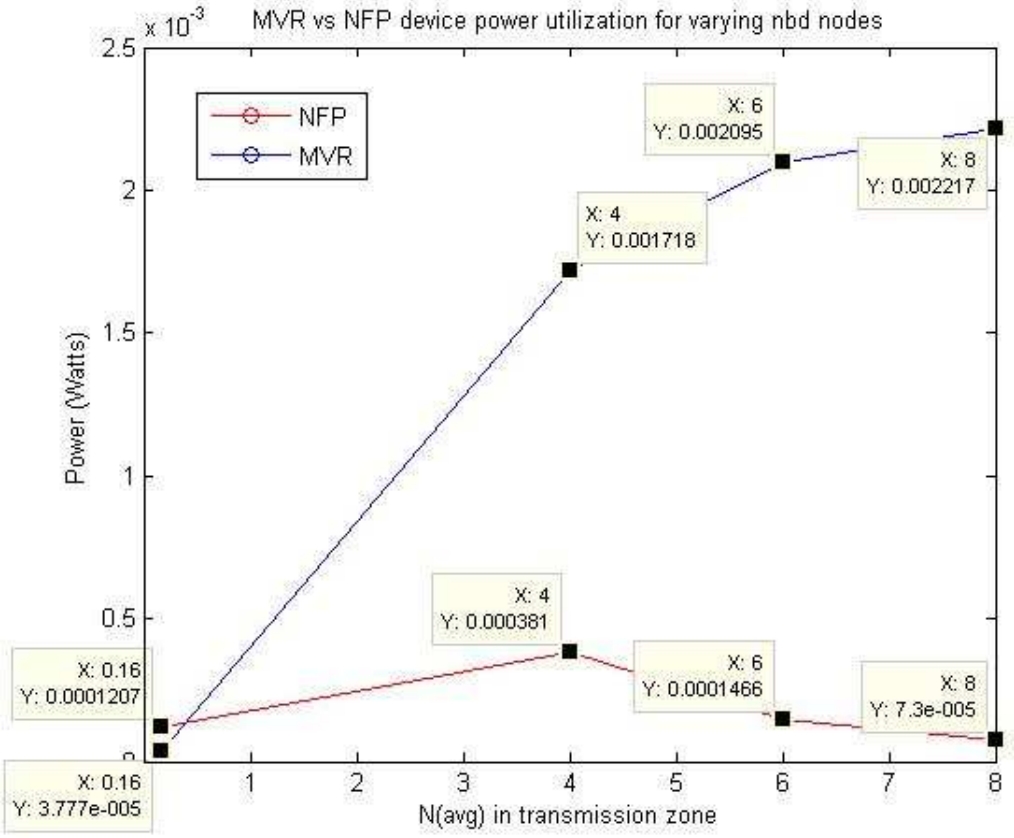

Figure 5.33: Device power utilized in NFP and MVR for various values of λ

Observations and Inferences from Fig 5.33 :-

- We can see that for higher values of Neighboring nodes, Device Power for MVR is much higher than that of NFP.
- But when N_{avg} gets very small, the situation changes. i.e there seems to exist a $\lambda_{critical}$ below which the MVR exhibits a better performance.
- According to this plot, the critical value of N_{avg} comes out to be 0.3., or $\lambda_{critical}$ = 9.55 * 10-4 m^{-2}.
- For this value of $\lambda_{cricitcal}$, the Device Power Consumed, obtained from the analysis equations were Pw_{NFP} = 0.1436*10^{-3} Watts and Pw_{MVR} = 0.1441*10^{-3} Watts

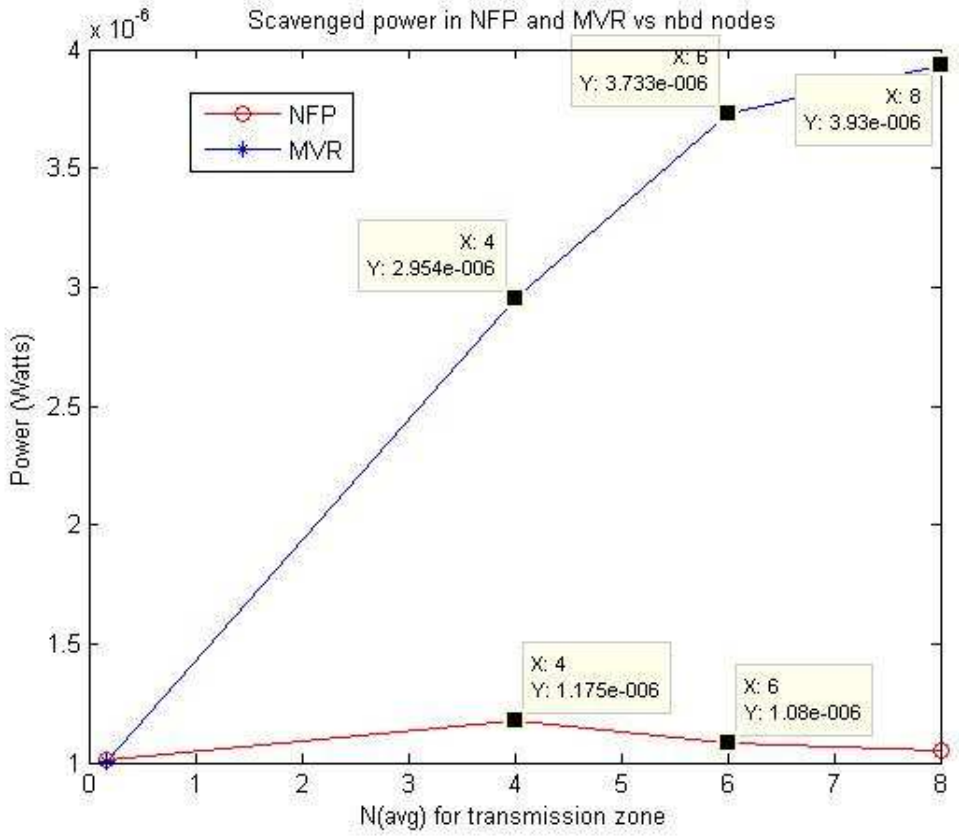

Figure 5.34: Scavenged power for NFP and MVR for various values of λ

Observations and Inferences from Fig 5.34 :-

- Energy Scavenged is the scalar sum of the Received Intended Signal Power and the Power from the interfering nodes.
- As is clear from our results, for scavenging purposes, MVR is quite better than NFP for higher values of N_{avg}.
- But, same as for Device Power, here also after a critical value of N_{avg} OR λ, the behavior changes.
- For Navg = 0.16, $PScvng_{NFP}$ = 0.1013*10^{-5} Watts and $PScvng_{MVR}$ = 0.1007*10^{-5} Watts.
- Thus, we can say that N_{avg} critical for energy scavenging is close to 0.16 , $\lambda'_{critical}$ = 5.09 * 10^{-4} m^{-2}.

Chapter 6

Conclusion

Non Power Control

We observed that the total value of interference for a fixed value of lambda actually peaks at the average node count in the effective interference area (navg). This was intuiutively expected as the probability of occurence of navg nodes is the maximum and one associate the maximum interference at that node count. The plots from the analysis have been reasonably verified by the results from brute force simulations. Overall, the best strategy in the case of non-power control is to choose the nearest possible node, since this results in the least interference at the immediate receiver and a high value of SIR. Also, it turns out that these parameters do not vary a lot with change in lambda. Therefore, a change in network node density won't cause any noticeable increase/decrease in the average retransmission rate or throughput.

Power Control

Compared with the non-power control, the curves for Int_1, Int_2, Int_3 and Int_Total prove to be very similar in shape for all the power-control transmission strategies. As was the intuition, the total interference (for a fixed lambda) at a receiver is the least for NFP among the three strategies. Also, NFP proves to be the best in terms of internal device power utilization , but only for higher values of λ. We obsereved that if the node density gets very sparse, (λ is very small,i.e. below the proposed $\lambda_{critical}$ = 9.55 * 10-4 m^{-2}) MVR gives a better Device Power Utilization. Also, it is evident from fig 5.35, that for higher λ device power utilization for NFP decreases and for MVR increases.

We also obsereved that, the random node selection process exhibits Device power utilization comparable to MVR for $N_{avg} = 4$. This suggests that we dont need spend energy on finding out the farthest node (or the need to know the distribution map of the nodes). We can randomly select a node and would get approx same device power utilization as that of MVR.

We also touched upon the Energy Scavenging problem and observed that MVR performed much better than NFP, but again only for higher values of λ. And below the proposed $\lambda^{'}_{critical}$ NFP gives a higher scavenged power than MVR. This $\lambda^{'}_{critical}$ = 5.09 * 10^{-4} m^{-2}.

Bibliography

[1] T.-C. Hou and V. O. K. Li, "Transmission range control in multihop packet radio networks," *IEEE Trans. Commun.*, vol. 34, no. 1, pp. 38–44, Mar. 1986.

[2] Swades De, "An Integrated Cross Layer Study of Wireless CDMA Sensor Netowks," in *IEEE Journal on Selected Areas in Communications*,vol. 22,no. 7,September 2004.

[3] Swades De. "On Hop Count and Euclidean Distance in Greedy Forwarding in Wireless Ad Hoc Networks," *Communications Letters, IEEE*, vol. 9, issue. 11, Nov 2005.

[4] K.Kopsa, Z.Mats,H.Artes and F.Halawatsch, "Bit Error Rate estimation for a joint detection receiver in the downlink of UMTS/TDD" , in *Proc. Mobile and Wireless Communication Summit 2003*,pp. 256–260, June 2003

[5] *http://www.chipcon.com/files/CC2420_Data_Sheet_1_2.pdf*, June 2004.

[6] R. Nagpal, H. Shrobe, and J. Bachrach, "Organizing a global coordinate system from local information on an ad hoc sensor network," in *Proc. Workshop on Information Processing in Sensor Networks*, Palo Alto, Apr. 2003, Springer LNCS, vol. 2634, pp.333–348.

[7] R. Hekmat and P. V. Mieghem, "Degree distribution and hop count in wireless ad hoc networks," in *Proc. IEEE ICON*, Sydney, Australia, Sept. 2003, pp. 603–609.

[8] L. Kleinrock and J. Silvester, "Optimum transmission radii for packet radio networks or why six is a magic number," in *Proc. IEEE National Telecomm. Conf.,*, Dec. 1978, pp. 4.3.1–4.3.5.

[9] H. Takagi and L. Kleinrock, "Optimal transmission ranges for randomly distributed packet radio terminals," *IEEE Trans. Commun.*, vol. 32, no. 3, pp. 246–257, Mar. 1984.

[10] A. Rao, C. Papadimitrou, S. Ratnasamy, S. Shenker, and I. Stoica, "Geographic routing without location information," in *Proc. ACM/IEEE MobiCom*, San Diego, CA, Sept. 2003, pp. 96–108.